5

ORNL-3077
UC-25 - Metals, Ceramics, and Materials

FABRICATION DEVELOPMENT OF UO_2-STAINLESS STEEL COMPOSITE FUEL PLATES FOR CORE B OF THE ENRICO FERMI FAST BREEDER REACTOR

J. H. Cherubini
R. J. Beaver
C. F. Leitten, Jr.

OAK RIDGE NATIONAL LABORATORY
operated by
UNION CARBIDE CORPORATION
for the
U.S. ATOMIC ENERGY COMMISSION

Printed in USA. Price $2.25. Available from the

Office of Technical Services
Department of Commerce
Washington 25, D.C.

ORNL-3077

Contract No. W-7405-eng-26

METALLURGY DIVISION

FABRICATION DEVELOPMENT OF UO_2-STAINLESS STEEL COMPOSITE FUEL PLATES FOR CORE B OF THE ENRICO FERMI FAST BREEDER REACTOR

J. H. Cherubini, R. J. Beaver, and C. F. Leitten, Jr.

DATE ISSUED

APR - 4 1961

OAK RIDGE NATIONAL LABORATORY
Oak Ridge, Tennessee
operated by
UNION CARBIDE CORPORATION
for the
U. S. ATOMIC ENERGY COMMISSION

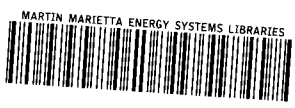

TABLE OF CONTENTS

FABRICATION DEVELOPMENT OF UO_2-STAINLESS STEEL COMPOSITE FUEL PLATES FOR CORE B OF THE ENRICO FERMI FAST BREEDER REACTOR

J. H. Cherubini, R. J. Beaver, and C. F. Leitten, Jr.[1]

ABSTRACT

The experimental work reported herein is concerned with the development of an inexpensive composite fuel plate with a high burnup potential for application in a 500°C sodium environment as Core B of the Enrico Fermi Fast Breeder Reactor. The dispersion fuel product resulting from an eighteen-month program of materials evaluation and fabrication studies at the Oak Ridge National Laboratory (ORNL) consists of 35 wt % spheroidal UO_2 dispersed in type 347B stainless steel powder and clad with wrought type 347 stainless steel. Nominal over-all dimensions of Type II design fuel plates are 18.97 in. long x 2.406 in. wide x 0.112 in. thick with 0.005-in. cladding. Reliable processing methods for achieving a uniform distribution of spheroidal UO_2 in the matrix powder and cladding the sintered powder compact by roll bonding are described. Examination of experimental plates reveal that the degree of UO_2 fragmentation and stringering encountered during processing is primarily a function of the degree of cold work employed in the finishing operation and the starting quality of the UO_2 powder. Cladding studies indicate that a sound metallurgical bond can be achieved with an 87.5% reduction in thickness at 1200°C and that close processing control is required to meet the stringent tolerances specified. The developed process meets all criteria except possibly the surface finish requirement; occasionally, pitting occurs due to scale embedded during hot working. Detailed procedures covering composite plate manufacture are presented.

INTRODUCTION

In the summer of 1959, a program was initiated at ORNL to develop an improved UO_2-stainless steel dispersion fuel element for use in Core B of the Enrico Fermi Fast Breeder Reactor. This fuel element was developed under the sponsorship of the AEC Power Demonstration Program in accordance with a design

---

[1] On loan to the Atomic Energy Commission Research Establishment, Risö, Roskilde, Denmark.

established by Atomic Power Development Associates (APDA). Included in the scope of the program were (1) the generation of technical data needed in support of the APDA design effort and (2) the establishment of reliable processing methods for producing composite fuel plates and fuel plate subassemblies. This report is concerned only with materials selection and processing of fuel plates; other aspects of the work will be covered in subsequent reports.

The UO_2-stainless steel dispersion concept was selected for Core B since the technology of this basic system was well-advanced, its irradiation stability was proven under the required operating conditions, and the costs of stainless steel base components was not prohibitive.[2,3] It was to serve as an interim fuel loading until a more advanced system of high-breeding capabilities could be developed.

The final fuel element design, shown in Fig. 1, stipulates a 0.112-in.-thick plate containing a fuel-bearing section of 2.2 x 18 x 0.102 in. containing 35 wt % UO_2 in type 347 stainless steel. During reactor operation, the bundle is cooled with sodium at 485°C and the nominal maximum fuel temperature in the plate is 560°C. The relatively high plate temperature compounded by a high, anticipated fuel burnup, 25% of the U^{235} atoms, preordained the use of relatively large-sized spheroidal UO_2 particles to minimize the possibility of structural damage from irradiation.

The general plate fabrication techniques were patterned after the methods established for manufacturing similar composite plates for the SM-1 Reactor at Ft. Belvoir, Virginia.[4] The procedures consisted of (1) weighing the required UO_2 and stainless steel for each compact, (2) blending the powders to obtain a uniform distribution of the fissile compound, (3) compacting at room temperature, (4) sintering in hydrogen, (5) coining at room temperature, (6) encapsulating in an evacuated stainless steel billet,

---

[2] V. O. Haynes et al., Summary of UO_2-Stainless Steel Dispersion Fuel Element Irradiation Experiments, ORNL-CF-58-2-71 (March 18, 1958).

[3] J. E. Cunningham et al., Fuel Dispersions in Stainless Steel Components for Power Reactors, Fuel Element Conference, Paris, November 18-23, 1957, TID-7546, Book I (March, 1958).

[4] J. E. Cunningham et al., Specifications for Fabrication Procedures for APPR-1 Core II Stationary Fuel Elements, ORNL-2649 (Jan. 29, 1959).

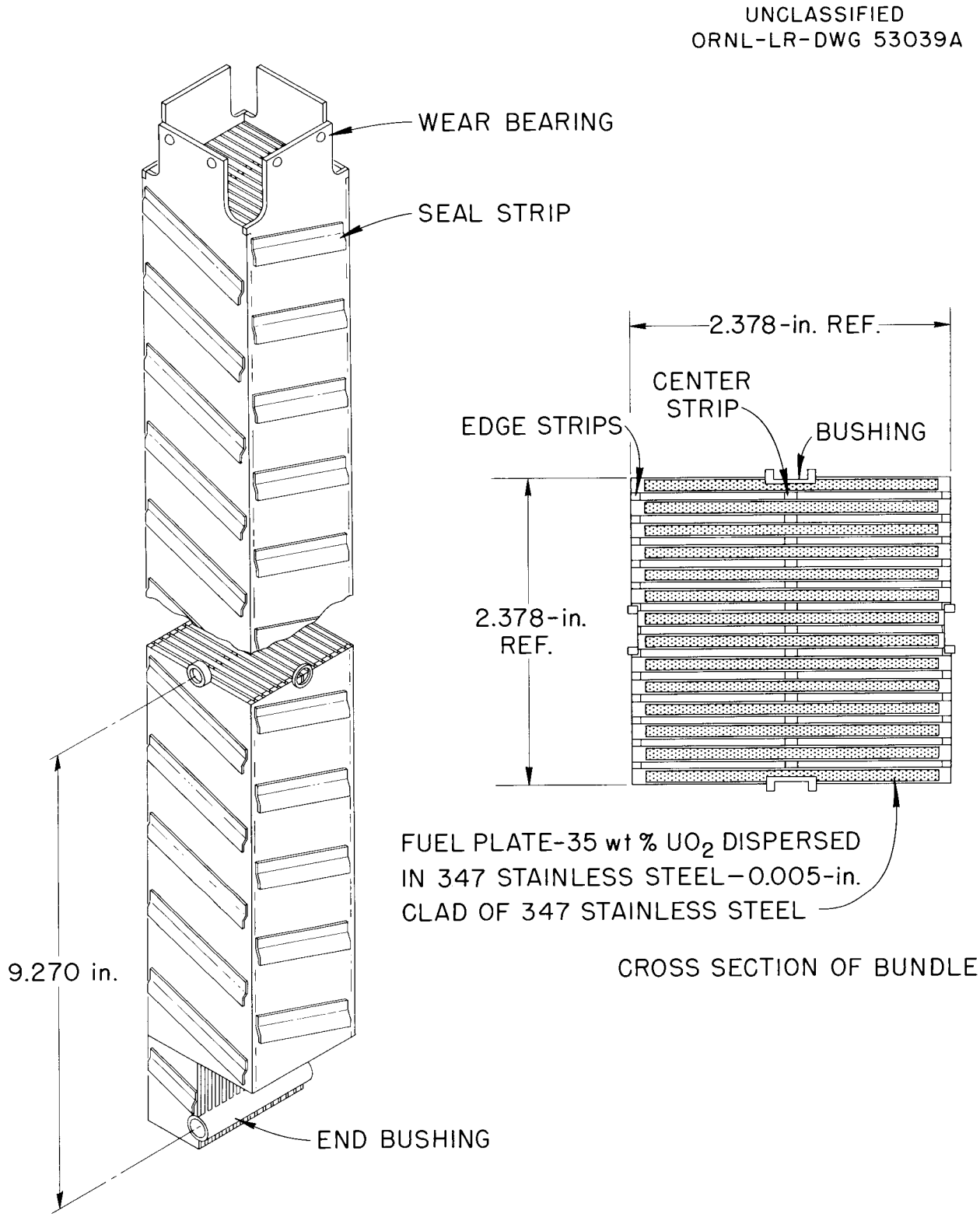

Fig. 1 Tentative Fuel Bundle Design for Core B of the Enrico Fermi Fast Breeder Reactor.

(7) hot rolling to obtain metallurgical bonding of the cladding to the fuel core and frame, and (8) cold finishing to specified size.

Although basic fabrication procedures were well established, several problems peculiar to the Core B fuel element remained to be resolved. One was to devise means for homogeneously incorporating the coarse spheroidal UO_2 particles in the stainless steel matrix. A variety of powder metallurgy blending schemes were assessed before a suitable technique was finally developed. Secondly, some concern existed as to whether appreciable difficulties would arise in roll cladding these thick fuel plates, particularly since the ratio of clad-to-core thickness was unusually small. However, preliminary plate fabrication studies readily allayed this concern. Experiments were also conducted to determine the least amount of cold rolling that could be employed consistent with dimensional and flatness requirements of the plates, while at the same time ensuring maximum integrity of the UO_2 particles. The fourth major problem was to establish whether or not the rigorous dimensional tolerances originally requested by APDA could be met. The reasonability of these specified dimensions was established by fabricating a quantity of prototype fuel plates. This culminating phase of the development demonstrated that the selected manufacturing procedures, although possibly not optimum, would consistently produce fuel plates of high quality.

PLATE DESIGN

Design criteria for fuel plates were established by APDA and represented tentative but desirable specifications. Initially, development of a composite plate meeting the dimensional requirements, shown in Fig. 2, was requested. Important dimensions include the 36-in. fuel section length, the 0.122-in. inactive edge of stainless steel, the 0.007-in. cladding thickness, and the ±0.003-in. tolerance on the 0.116-in. total plate thickness. This tolerance was tentatively assigned because the composite was to be finished by hot rolling to preserve, as nearly as possible, the spheroidal character of the UO_2. This plate design was designated as Type I.

A subsequent change in fuel element concept necessitated a modification of plate dimensional specifications to the Type II design shown in Fig. 3. The principal differences between the Type II and the Type I plate designs are decreases in (1) fuel section length to 18 in., (2) the inactive stainless

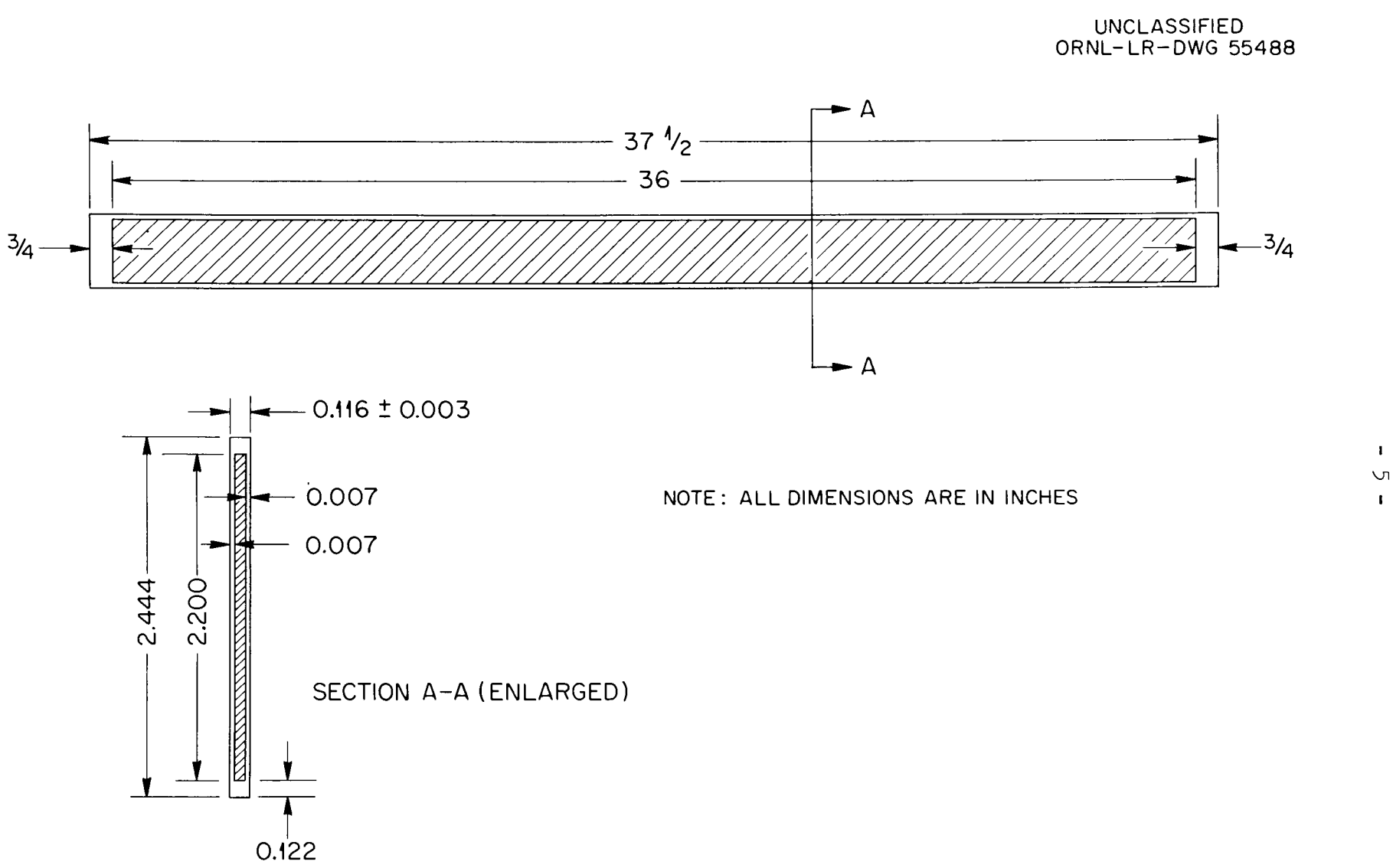

Fig. 2 Dimensioned Drawing of Type I Fuel Plates.

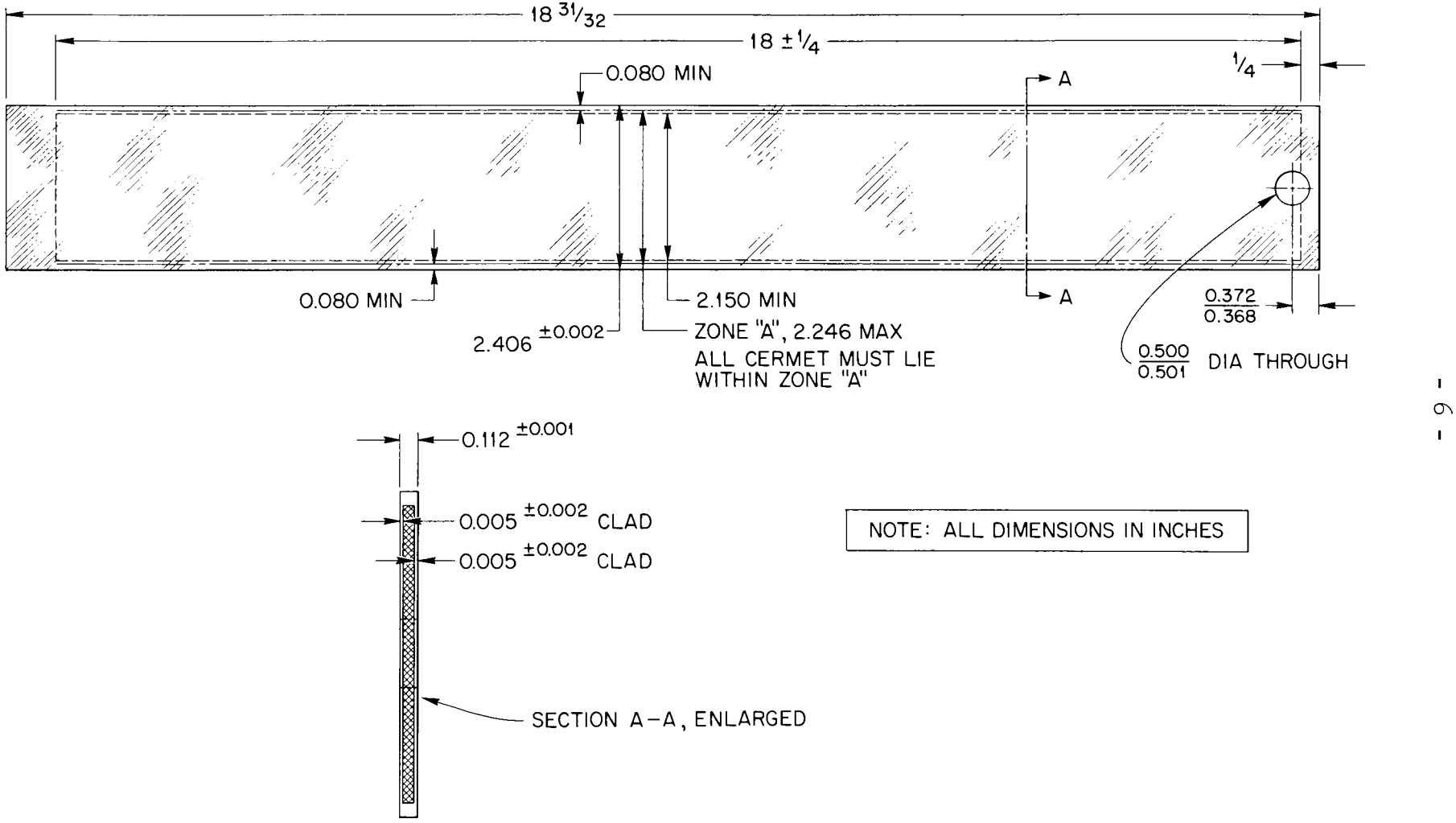

Fig. 3 Dimensioned Drawing of Type II Fuel Plates.

steel plate edges to 0.080 in., (3) the cladding thickness to 0.005 in., and (4) the plate thickness to 0.112 in. The tolerance of ±0.001 in. on the plate thickness dictated cold reduction to finished dimensions, with the attendant degradation of the UO_2 particles. The average cladding thickness is specified at 0.005 in. ± 0.001; however, the actual thickness may be a minimum of 0.003 at any specific point. Pertinent design data for both types of plates are summarized in Table 1.

SELECTION OF MATERIALS

Spheroidal UO_2 in the size range of 105–149 μ (-100 +140 mesh) was selected as the fuel most desirable for application in Core B of the Fermi reactor. The selection was based on the postulate that the resistance of UO_2-stainless steel dispersion to irradiation damage can be improved by increasing the mean free path between the centers of the UO_2 particles.[5] It is obvious that for any specific particle size and concentration, a dispersion of spherical particles maximizes the mean free path between the particle centers. Furthermore, the spheroidal shape provides a more favorable geometry to resist swelling of the individual fuel particles due to fission product buildup.

Oxides produced by various commercial vendors were procured and examined for microstructural characteristics before and after fabricated into composite plates. A detailed report covering this phase of the investigation will be issued in the near future.

In general, though, it was found that UO_2 of relatively low bulk density fragmented and stringered extensively in roll-clad composite plates. Uranium dioxide of high bulk density resisted fragmentation and retained a high degree of spheroidicity. These effects may be seen in the comparison shown in Fig. 4.

Austenitic stainless steel was selected as the cladding and matrix material of the composite fuel plate, although the particular type was not chosen until pertinent elevated-temperature properties of types 347, 310, and 316 stainless steel were reviewed. It was expected that sigma phase would form in those regions of the fuel operating near the nominal maximum

---

[5] H. M. Finniston and J. P. Howe (eds.), Metallurgy and Fuels in Progress in Nuclear Energy [5] 2, 295–362, Pergamon Press, 1959.

TABLE 1

SUMMARY OF PERTINENT DESIGN DATA

		Type I Plate	Type II Plate
I.	GEOMETRY		
	Plate length, in.	37.7	18.97
	Plate width, in.	2.450	2.406
	Fuel core length, in.	36	18 ± 0.25
	Fuel core width, in. (min)		2.150
	Effective fuel core width, in. (max)	2.200	2.246
	Average cladding thickness, in.	0.007	0.005 ± 0.001
	Minimum cladding thickness, in.	0.005	0.003
	Fuel core thickness, in.	0.102	0.102
	Total plate thickness, in.	0.116 ± 0.003	0.112 ± 0.001
II.	MATERIALS		
	Cladding		
	Type of stainless steel	347	347
	Framing		
	Type of stainless steel	347	347
	Fuel Core		
	Number of cores per fuel plate	4	2
	Uranium dioxide		
	particle shape	spherical	spherical
	particle size (mesh)	-100 +140	-100 +140
	weight, grams per plate	364.56	182.28
	Stainless steel		
	type	347B*	347B*
	size (mesh)	-100	-100
	weight, grams per plate	720.20	342.80
	Concentration of UO_2		
	weight percent	33.6	36.1
	volume percent	26.7	27.7

*Refers to type 347 with 2% silicon addition.

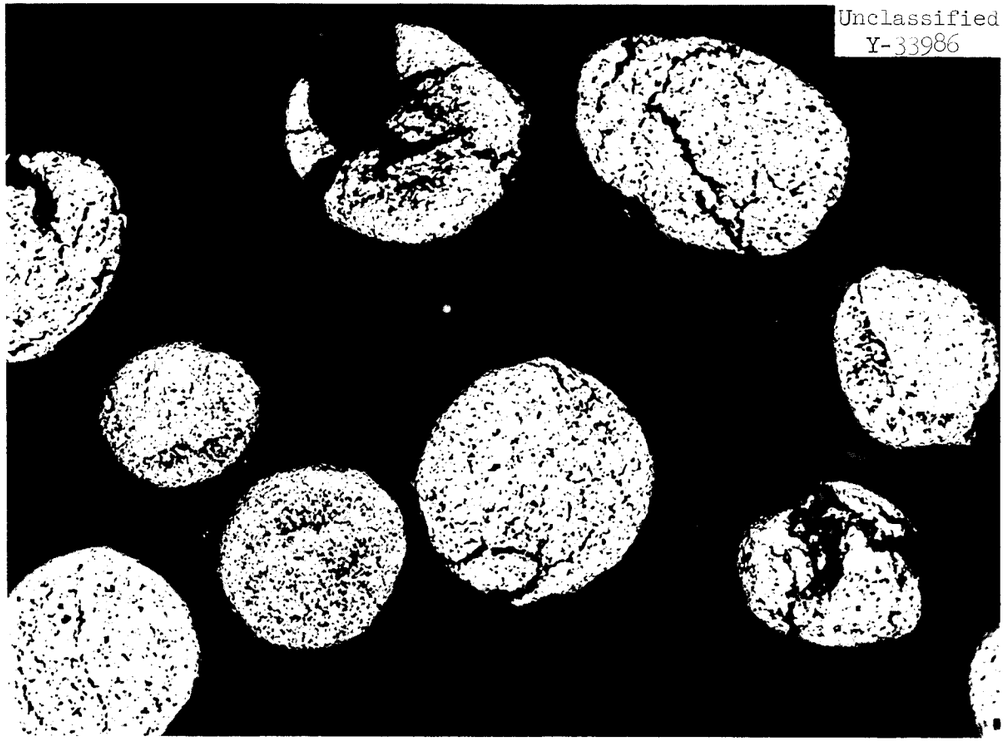

(a) Poor Quality UO_2 as Received from Vendor. As polished. 250X.

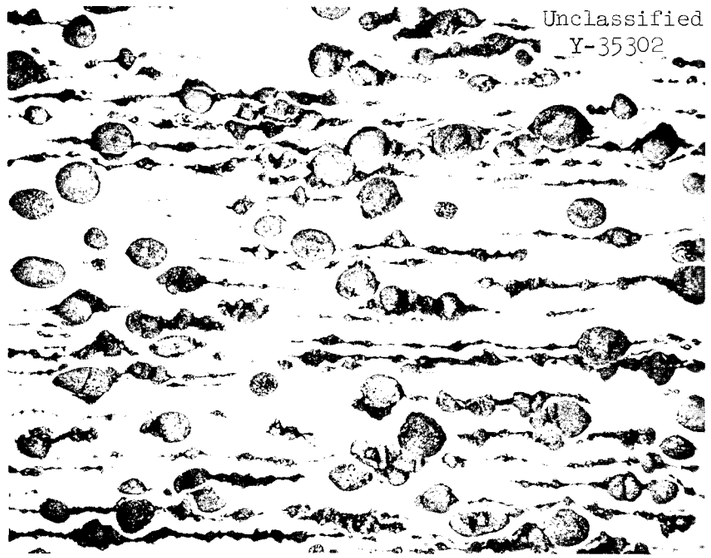

(b) Poor Quality UO_2 Dispersed in Fabricated Plate. Etchant: Aqueous solution of 10% HNO_3-H_2O_2. 50X.

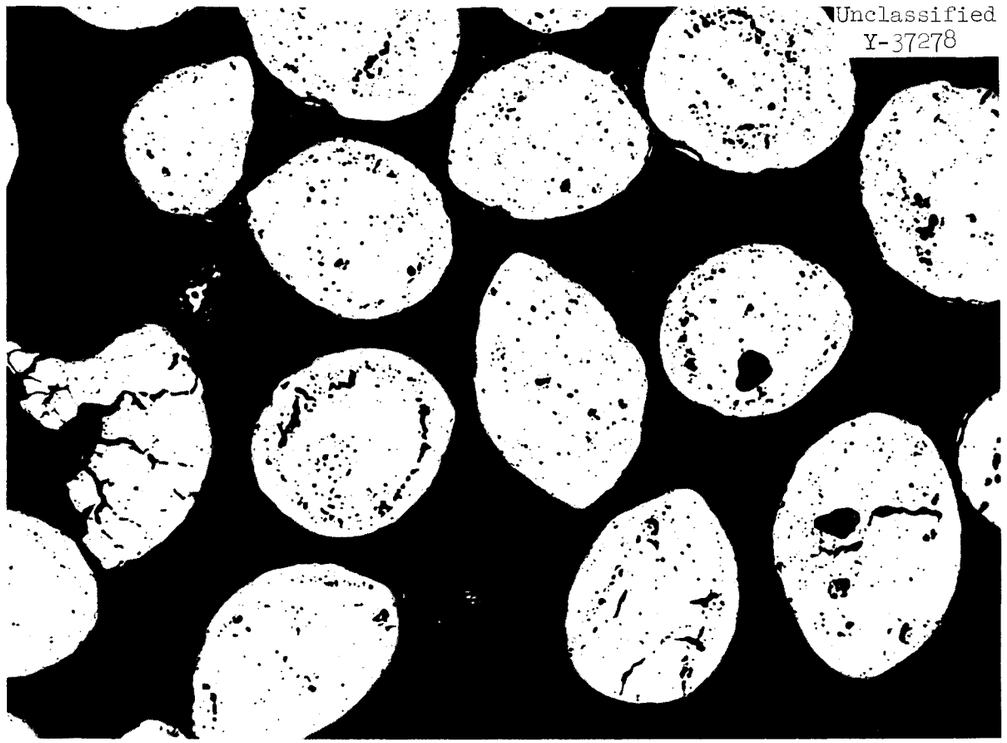

(c) Good Quality UO_2 as Received from Vendor. As polished. 250X.

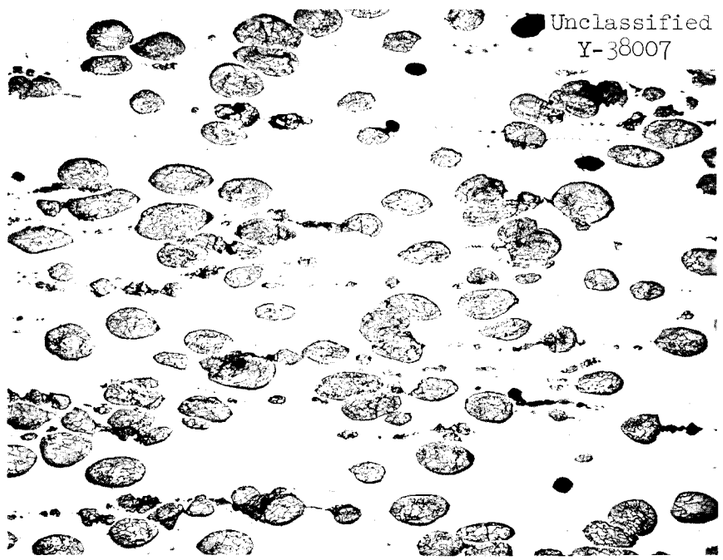

(d) Good Quality UO_2 Dispersed in Fabricated Plate. Etchant: Aqueous solution of 10% H_2SO_4-20% H_2O_2. 50X.

Fig. 4 Comparison of the Quality of Two Batches of Spheroidal UO_2

temperature of 560°C. Data presented in Table 2 indicate that reductions in

TABLE 2

ROOM-TEMPERATURE PROPERTIES OF STAINLESS STEELS AFTER EXPOSURE AT 1050°F*

Stainless Steel Type	Impact Strength (ft-lb)			Tensile Ductility (Percent Reduction of Area)	
	Unexposed	1,000 hr	10,000 hr	Unexposed	10,000 hr
316	80	72	49	78	69
347	56	55	51	72	73
310	75	48	29	70	54

*"Pipe and Tubes for Elevated Temperature Service," National Tube Division of U. S. Steel Bulletin No. 26, 59th ed.

impact strength and tensile ductility are not as great with type 347 stainless steel as with the other two types of stainless steels evaluated. In addition, type 347 stainless steel has a yield strength at 560°C which is approx 20% higher than either type 310 or 316.(ref 6) Since irradiation damage theory predicts that resistance to damage is a function of matrix strength,[7] and since its sigma-forming potential appears to be less, type 347 stainless steel was ultimately selected as the cladding and matrix material for the Core B fuel plates.

PRELIMINARY INVESTIGATION OF PROCESS PARAMETERS

Fuel Core Homogeneity

A dependable procedure capable of producing homogeneous mixtures of 35 wt % -100 +140 mesh spheroidal UO_2 and stainless steel powder is a prerequisite for fuel plate manufacture. However, the nature of the powders

[6] Steels for Elevated Temperature Service, U.S. Steel Corporation, 1953.

[7] J. R. Weir, A Failure Analysis for the Low-Temperature Performance of Dispersion Elements, ORNL-2902 (May 27, 1960).

selected, including their shape, size, and density differences, favors classification within such a mixture. To abrogate this, various blending techniques were studied. The effects of blending sequence, stainless steel particle size distribution, and blending additive were examined. An oblique-type blender was used to prepare all powder mixes.

Each blended mixture consisting of 47 g UO_2 and 92 g stainless steel was compacted, sintered, coined, and roll clad into a composite plate. Any segregated regions originally present in the powder compact were evident upon examination of radiographs of the corresponding plate. It is noteworthy that the rolled plates contained a relatively thin fuel section, 0.045 in., in order to intentionally aggravate segregated regions which might be overlooked upon radiographic examination of the 0.102-in.-thick fuel section of a prototype plate.

The experimental results compiled from approx 100 roll-clad plates are summarized in Table 3. The simplest approach--blending the mixture without additives--was not successful despite radical changes in stainless steel particle size. Plates with the typical swirl segregation pattern illustrated in Fig. 5 resulted. The same pattern was typical when a dry additive of Carbowax 4000 was added in amounts of either 0.14 or 1.4 g per compact.

Additions of lauryl alcohol, ranging in amount from 0.15 to 0.30 cc per compact, gave variable results. Of thirty plates fabricated under the same conditions, approx 50% had acceptable homogeneity. The balance exhibited either a swirl pattern or a blotched pattern, which is illustrated in Fig. 6. In view of the variable results, lauryl alcohol was not considered to be a suitable additive.

Additions of Polyox 301 solution ranging from 0.10 to 0.20 cc per compact also resulted in blotched patterns.

It was generally noted that swirl patterns were associated with either dry blending or a solid additive. The blotched pattern was most frequently associated with the liquid additive.

It was subsequently felt that the variations in homogeneity of blends were due, at least in part, to classification during transfer and manipulation in the pressing die. This suggested pressing a wet, pasty mixture which would

TABLE 3

SUMMARY OF BLENDING EXPERIMENTS CONDUCTED TO PREPARE HOMOGENEOUS DISPERSIONS OF 35 Wt % SPHEROIDAL UO_2 IN TYPE 347 B STAINLESS STEEL

UO_2 Particle Size - 105/149μ

Blending Experimental Group	Stainless Steel Size Fraction (mesh)	Initial Blending Time (hr)	Type of Addition	Quantity of Addition	Reblend Time (hr)	Radiographic Evaluation of Homogeneity
A	a. -100 b. -325 c. -100 +325 d. -80 +120	3	None	None	None	Unacceptable homogeneity because of swirl patterns.
B	a. -100 b. -325 c. -100 +325	3	Carbowax 4000	0.14 g	None	Unacceptable homogeneity because of swirl patterns.
C	a. -100 b. -325 c. -100 +325	3	Carbowax 4000	1.4 g	None	Unacceptable homogeneity because of swirl patterns.
D	a. -100 b. -325 c. -100 +325	3	Lauryl alcohol	0.15 to 0.3 cc*	None	Unacceptable homogeneity because of blotch patterns.
E	-80 +120	1	Lauryl alcohol	~0.3 cc*	2	Erratic homogeneity. Generally a swirl pattern was observed.
F	a. -100 b. -325	1	Lauryl alcohol	0.15 to 0.3 cc*	2	Erratic regardless of stainless steel particle size or quantity of addition. Approx 50% of the plates were unacceptable because of blotch patterns.
G	a. -100 b. -325 c. -100 +325	1	Aqueous solution of 1.5 wt % Polyox 301	0.10 to 0.20 cc*	2	Unacceptable homogeneity because of blotch patterns.
H	a. -100 b. -325 c. -100 +325	1	Aqueous solution of 15 wt % Polyox 301	0.10 to 0.20 cc*	2	Unacceptable homogeneity because of blotch patterns.

(continued)

TABLE 3 (continued)

Blending Experimental Group	Stainless Steel Size Fraction (mesh)	Initial Blending Time (hr)	Type of Addition	Quantity of Addition	Reblend Time (hr)	Radiographic Evaluation of Homogeneity
I	-100	1/2	5% paraffin in CCl_4	0.15 1–7 cc**	1**	Acceptable homogeneity. Small elliptical areas of low uranium concentration observed in a few instances.
J	-325	1/2	5% paraffin in CCl_4	0.15 1–3 cc**	1-1/2 1/2**	Frequency of small elliptical areas of low uranium concentration increased with change to -325 mesh stainless steel powder.

*One squirt with atomizer is equivalent to 0.05 cc of additive.

**Blended dry for 1/2 hr, 0.15 cc added; reblended 1-1/2 hr, larger additions made, reblended 1/2 hr.

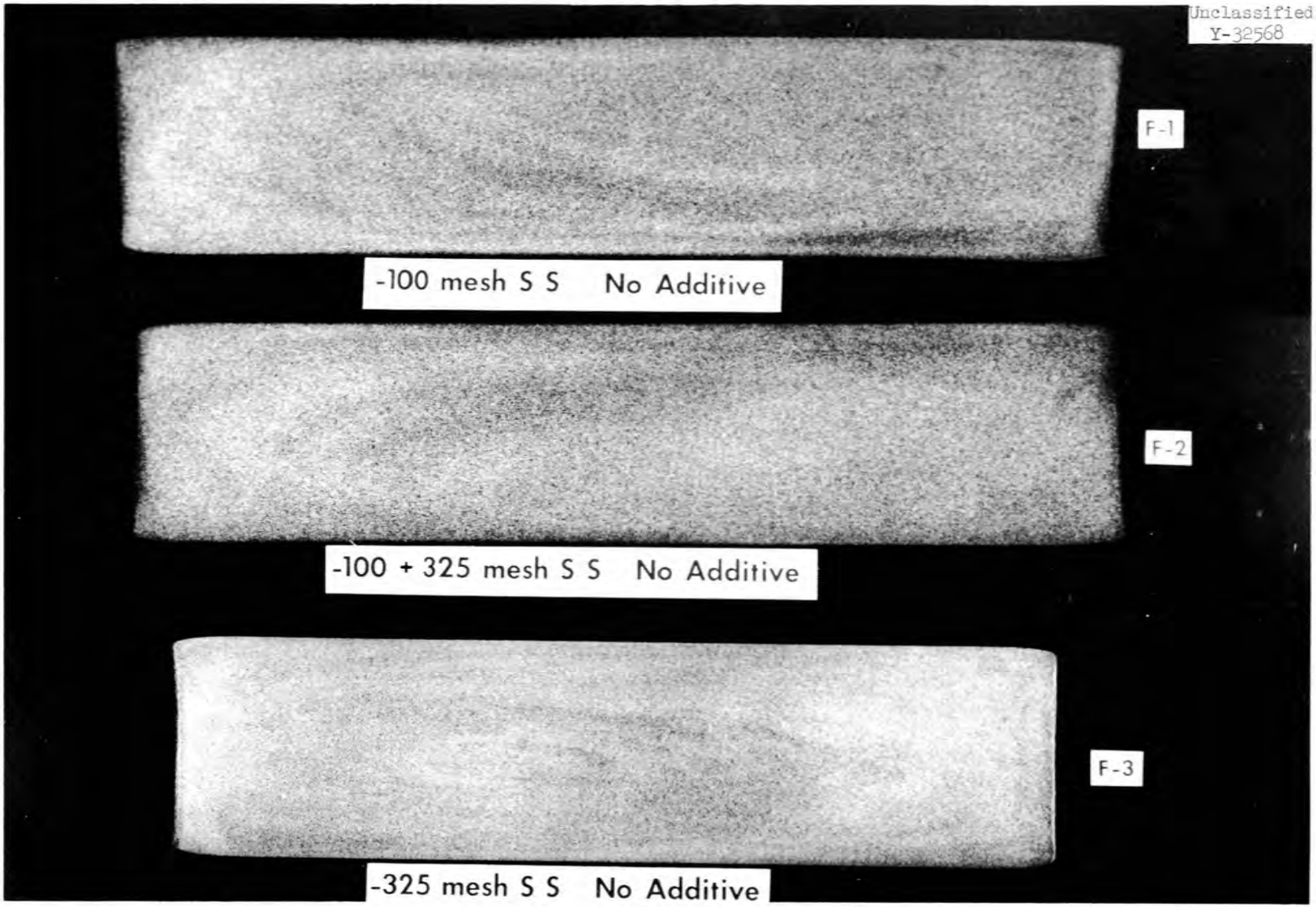

Fig. 5 Typical Swirl Segregation Patterns in Fuel Sections of Fabricated Plates Containing Compacts Blended with no Additive. Reduced 70% for reproduction.

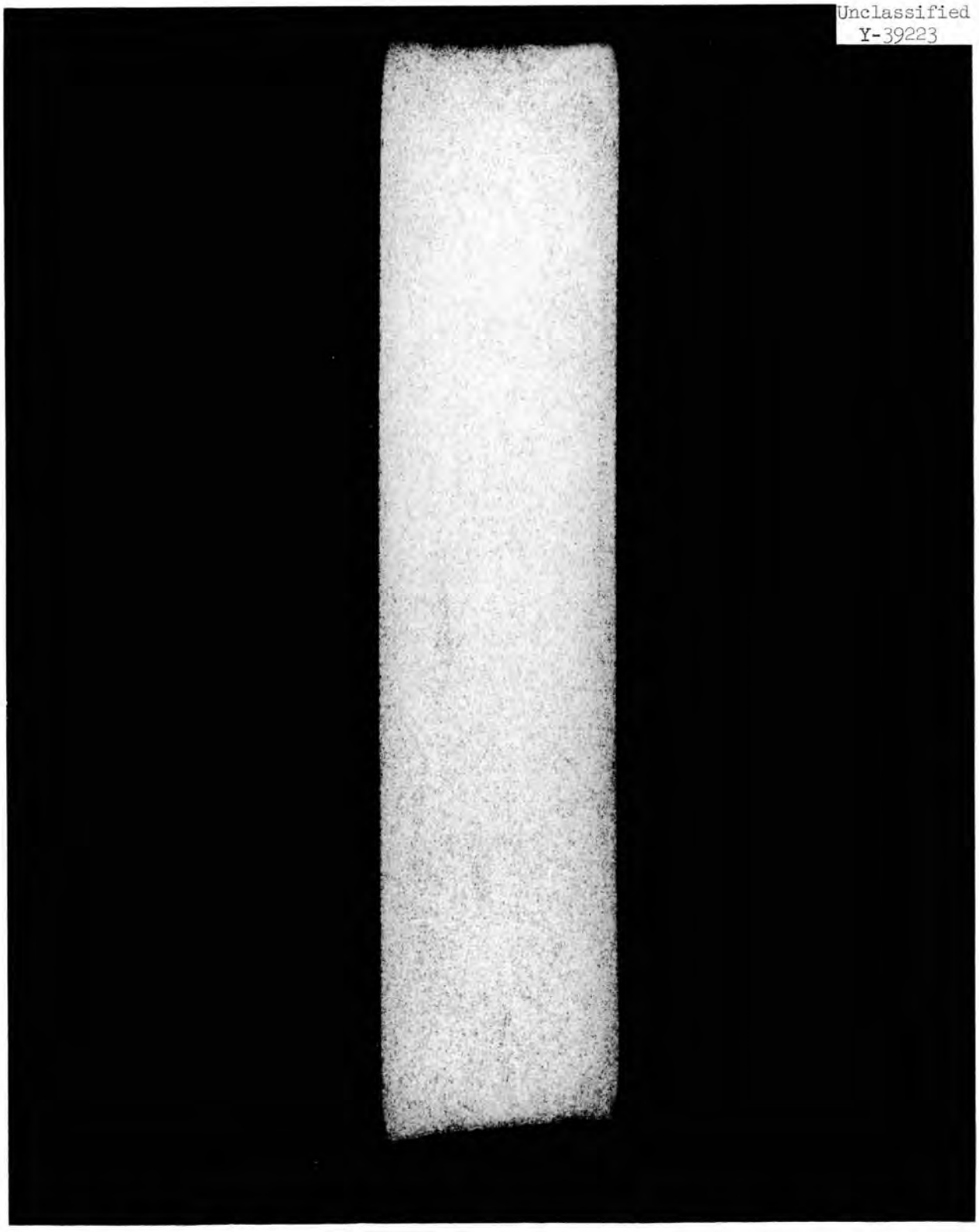

Fig. 6 Typical Blotch Segregation Patterns in Fuel Section of Fabricated Plate (F 50) Containing Compacts Blended with Small Additions of Lauryl Alcohol. Reduced 70% for reproduction.

have little opportunity to segregate between blending and pressing into a compact. Experiments were conducted with a solution of 5% paraffin in carbon tetrachloride as an additive. Results were encouraging and the following "paste blending" procedure was ultimately adopted:

1. Dry blend 90 g of -100 +140 mesh UO_2 and 180 g of -100 mesh stainless steel for 1/2 hr.
2. Add 0.15 cc of the 5% paraffin-carbon tetrachloride solution with an atomizer.
3. Reblend 1/2 hr.
4. Add 7 cc of the 5% paraffin-carbon tetrachloride solution with a syringe.
5. Reblend for 1/2 hr.

Typical homogeneity of the UO_2 in a fabricated fuel plate containing a fuel core prepared with this technique is illustrated in Fig. 7. Substitution of -325 mesh stainless steel powder in this procedure resulted in cores with small segregated regions indicating that the larger size stainless steel is more compatible in this process.

To ascertain the resistance of the paste blend to classification, a typical mixture was vibrated for 1 min prior to pressing into a compact. The UO_2 in the resulting roll-clad plate, No. F-89, was uniformally dispersed demonstrating that the paste-blended mixture did resist classification.

The homogeneity of the plates containing fuel sections prepared by paste blending was quantitatively assessed by chemical analysis of 3/4-in. square samples sheared from the fabricated fuel plates. The location and identity of the specimens are shown in Fig. 8 and the analytical results are summarized in Table 4. In the three plates examined, the maximum standard deviation of the uranium concentrations was ±0.102 wt % uranium.

Roll Bonding

Roll bonding was selected as the method for cladding stainless steel to the fuel core and frame because of the broad experience in cladding iron-base composites, its reliability, and recent experience in cladding stainless

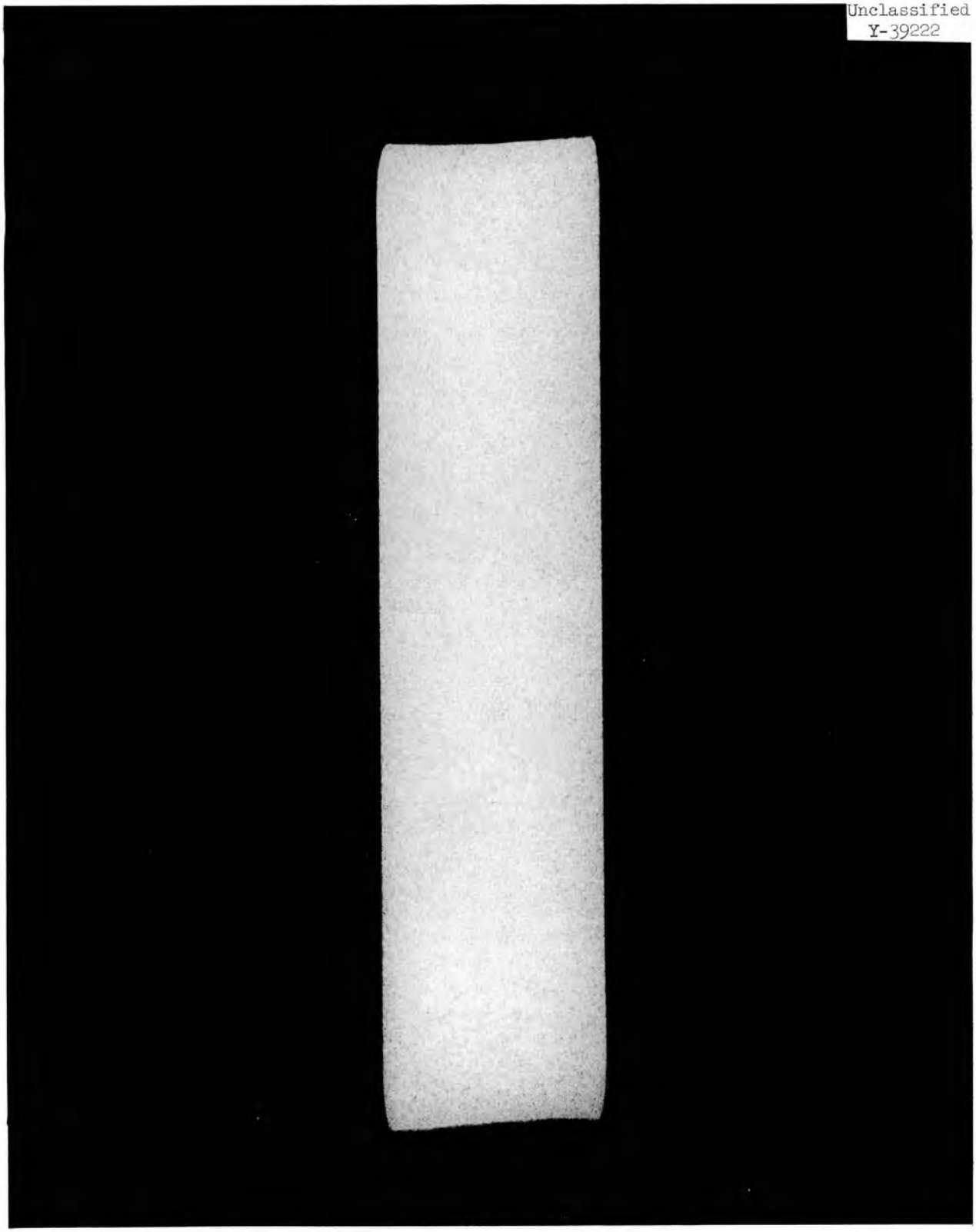

Fig. 7 Typical Homogeneity Pattern in Fuel Section of Fabricated Plate Containing Compacts Blended Using Paste Technique. Reduced 70% for reproduction.

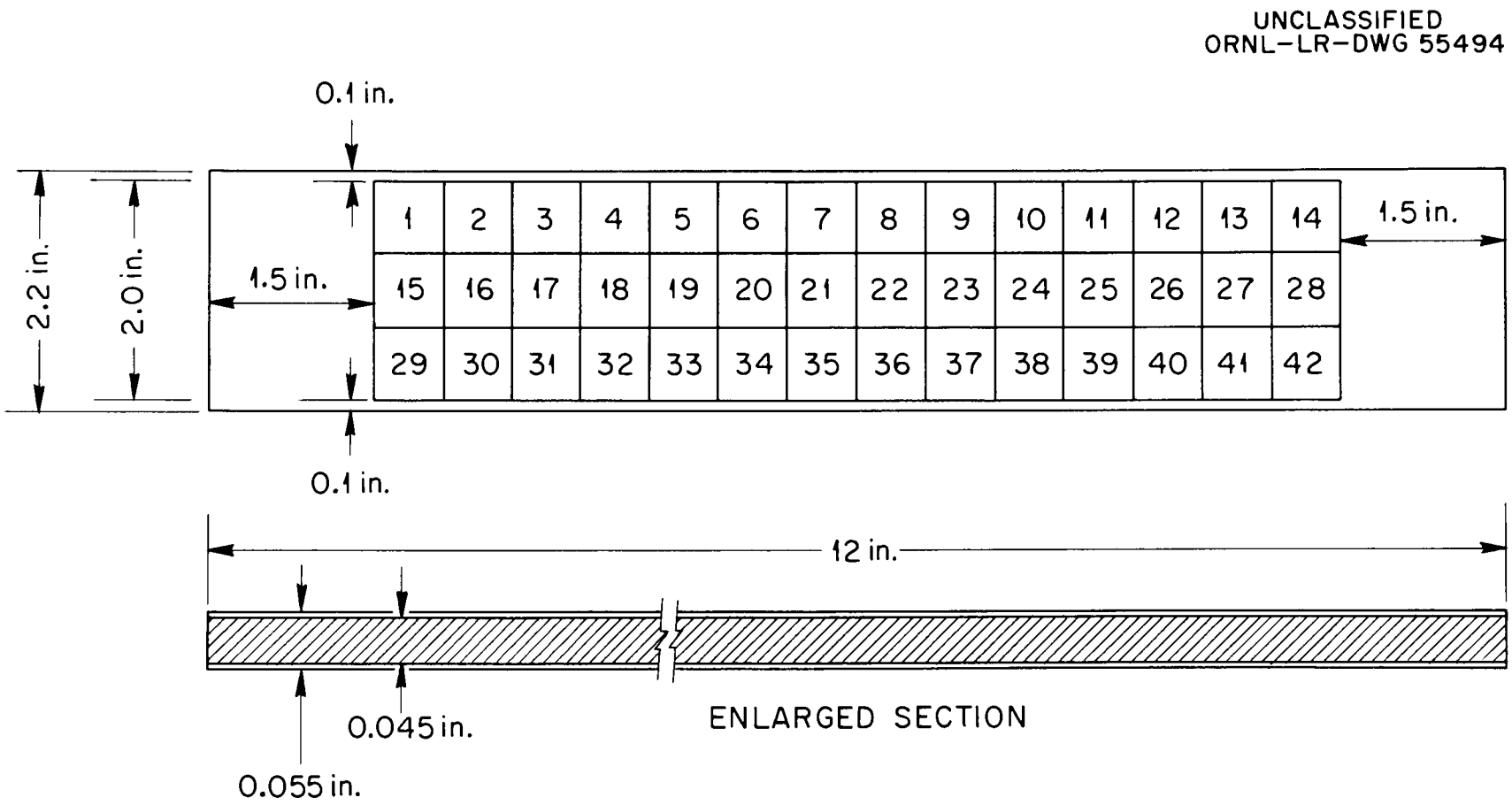

Fig. 8 Dimensioned Drawing of Fuel Core Section Showing Sampling Pattern for Uranium Analysis to Determine Homogeneity.

TABLE 4

URANIUM DISTRIBUTION IN COMPOSITE PLATES
CONTAINING 33 Wt % UO_2-STAINLESS STEEL DISPERSIONS

Plate No. F-80		Plate No. F-83		Plate No. F-89	
Sample No.	Wt % U*	Sample No.	Wt % U*	Sample No.	Wt % U*
8	21.76	14	21.13	1	21.72
14	21.54	15	22.04	2	21.46
16	21.42	17	22.12	10	21.76
20	21.38	19	21.88	11	21.60
25	21.74	21	21.95	17	21.19
31	21.47	23	21.60	18	21.58
33	21.62	25	21.80	23	21.58
37	21.76	27	21.78	24	21.57
		33	21.48	33	21.44
				34	21.72
				38	21.58
				40	21.72
				41	21.37
Average	21.59		21.75		21.56
Standard Deviation	0.059		0.102		0.045

*Includes dilution effect of stainless steel cladding.

steel to dispersions of UO_2 in stainless steel.[8,9] To determine the minimum total reduction compatible with reliable bonding, the self-bonding characteristics of unevacuated billets of type 347 stainless steel were determined as a function of total reduction in thickness by hot rolling at 1200°C. The results are summarized in Fig. 9. Grain growth across the original interfaces occurred at the three reductions examined, 70.6, 78.3, and 83.5%. However, the extent of bond-line contamination, consisting of both voids and nonmetallic inclusions, was clearly evident and erratic at reductions of less than 83.5%. To provide additional insurance of satisfactory bonding in the prototype plate, evacuated billets were used and the total hot reduction in thickness increased to 87.5%. The resulting bonding of a hot-rolled prototype plate is shown in Fig. 10. A similar plate, after a flatten-anneal cycle of 2 hr at 1150°C, is shown in Fig. 11. Although some grain growth has occurred, the size of the grains in the cladding are less than the cladding thickness.

Cold Rolling

Effect on Fuel Section

Since previous work at this laboratory revealed that cold working has a deleterious effect of UO_2 particles dispersed in stainless steel, experiments were conducted to determine the effects of 2 to 30% cold reduction on the structural behavior of the UO_2 particles.[8] As illustrated in Fig. 12, the spherical oxide cracked at a cold reduction of 2%, although stringering of the fissile phase was negligible at reductions of less than 10%. As the total reduction was increased, the frequency and size of the cracks changed proportionately and, above 20% reduction, exaggerated stringering of the fissile compound was realized.

---

[8] J. E. Cunningham et al., Fuel Dispersions in Stainless Steel Components for Power Reactors, Fuel Element Conference, Paris, November 18–23, 1957, TID-7546, Book I (March, 1958).

[9] L. C. Grimshaw, "Stainless Clad Steels," Metals Handbook (ed. by Taylor Lyman) p.545, The American Society for Metals, Cleveland, Ohio, 1948.

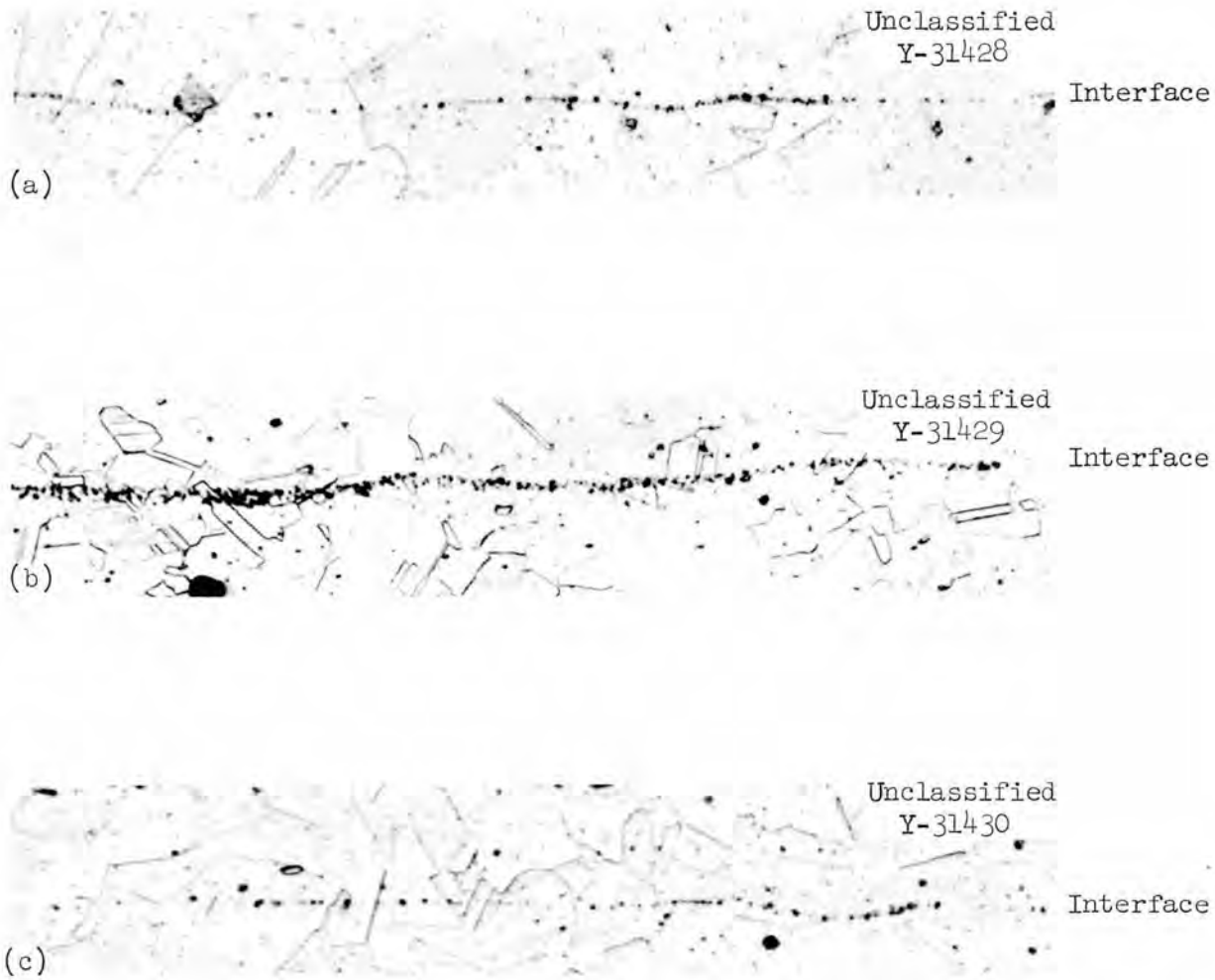

Fig. 9 Mating Interfaces Between Type 347 Stainless Steel Sheets as a Function of Reduction in Thickness at 1200°C (a) 70.6% reduction, (b) 78.3% reduction, (c) 83.5% reduction. Etchant: Glyceria regia. 500X.

Fig. 10 Bonding of Type 347 Stainless Steel Cladding to Type 347B Stainless Steel Matrix in Prototype Composite Plate. Hot-rolling temperature, 1200° C. Reduction in thickness, 87.5%. Longitudinal section. 200X.

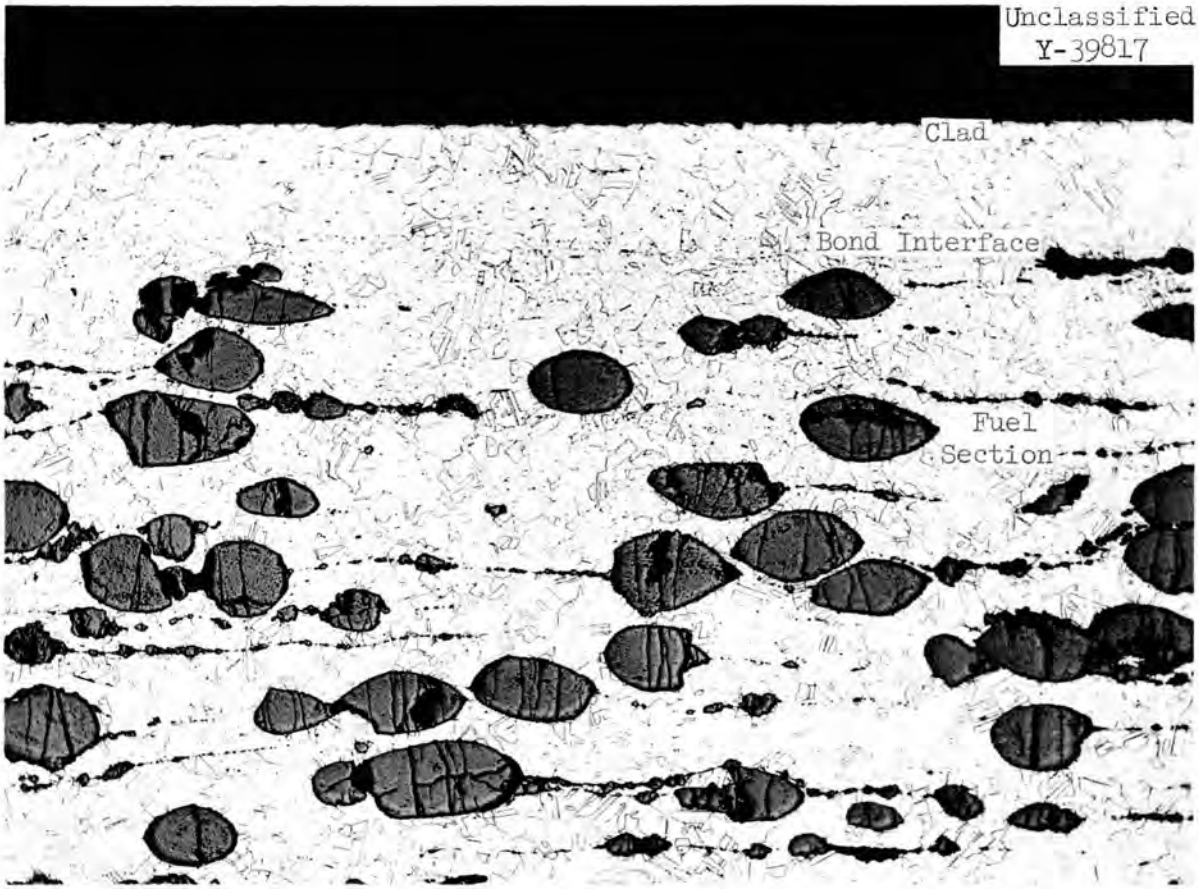

Fig. 11 Bonded Interface and Grain Size of Cladding in Type II Fuel Plate Annealed for 2 hr at 1150°C. Longitudinal section. 100X.

UNCLASSIFIED
PHOTO 52670

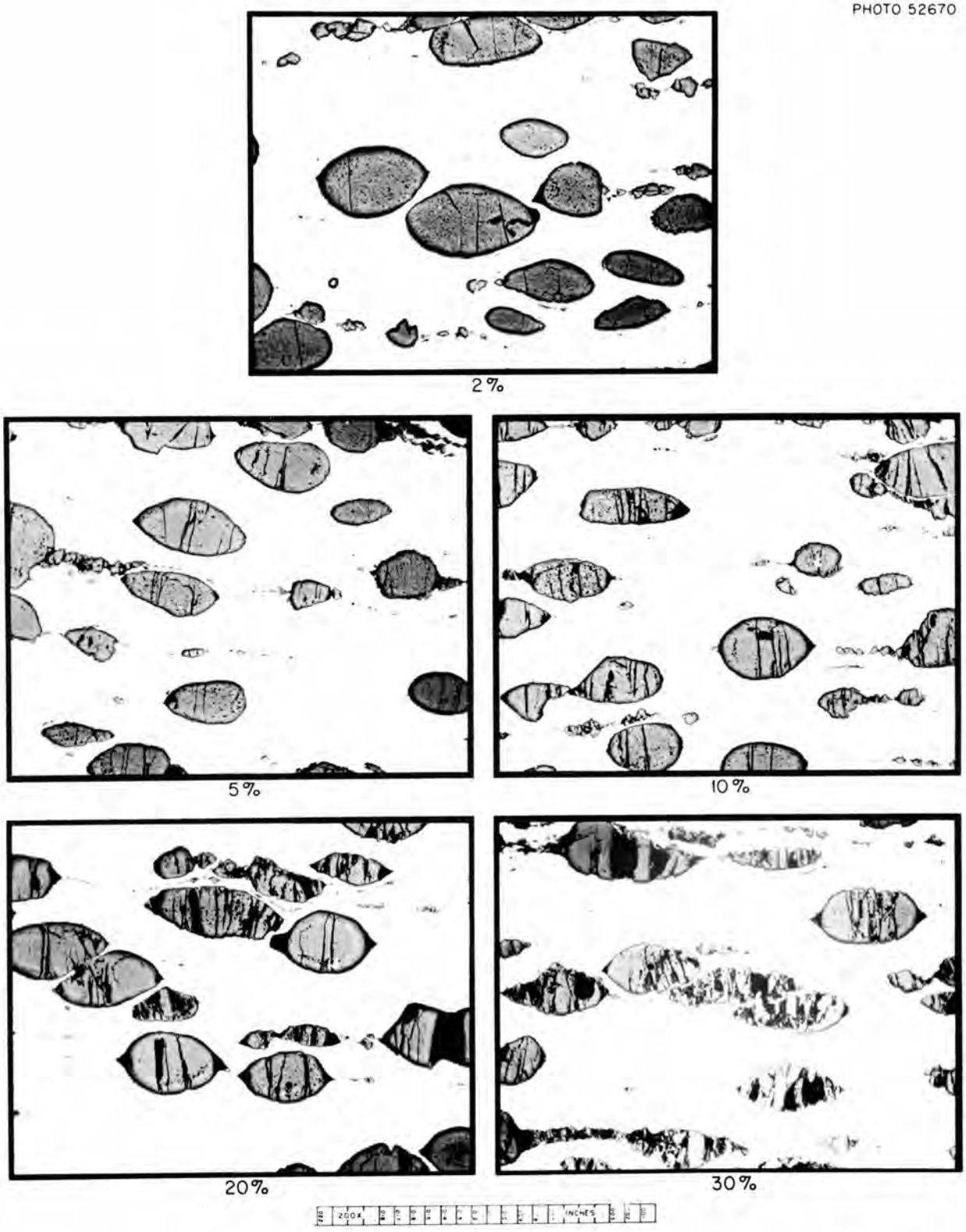

Fig. 12 Effect of Total Cold Reduction on UO_2 Particle Geometry (Batch A-534). 200X.

As might be expected, fracturing of the oxide results in a density decrease of the UO_2-stainless steel material. This relationship is illustrated in Fig. 13. Assuming density values of 10.97 g/cc for UO_2 and 7.91 g/cc for stainless steel, the theoretical density of the fuel section decreased from 94.07 to 91.93% when the plate was cold reduced 20% in thickness. Qualitatively similar relationships would be anticipated regardless of the particular batch of UO_2 contained in the cermet.

Effect on Plate Geometry

Cold rolling under certain conditions can cause rippling of the fuel plate. If excessive, such undulations are difficult to eliminate during subsequent flatten-annealing treatments. Therefore, a relatively flat as-rolled plate is a prerequisite to the attainment of a high-quality end product. Consequently, wrought type 347 stainless steel sheet, of the same geometry as composite plates, was cold rolled and the effect of roll design and total reduction on rippling was assessed.

Plates rolled through a 20-in.-diam x 30-in.-face 2-high Mesta Mill maintained acceptable flatness at total reductions ranging from 2 to 20%, as illustrated in Fig. 14. A similar series of plates rolled through a 4-high Bliss Mill, equipped with 5-in.-diam work rolls and 12-in.-diam x 12-in.-face backup rolls, is shown in Fig. 15. Severe plate distortion at the lowest reduction examined, 2%, persisted until the total reduction approached 30%. In all cases, SAE 90 oil was used as the lubricant.

In confirmation of these observations, Type I prototype plates were cold reduced 3.5% in thickness on both the 2-high Mesta Mill and the 4-high Bliss Mill and subsequently flat annealed. As anticipated, the plate rolled through the large diameter rolls was considerably flatter than the other as shown in Fig. 16.

As a final compromise to control flatness, minimize UO_2 fragmentation, and maintain plate thickness to ±0.001 in., a cold reduction of 3 to 5% executed with 20-in.-diam work rolls was incorporated into the Type II plate fabrication procedure.

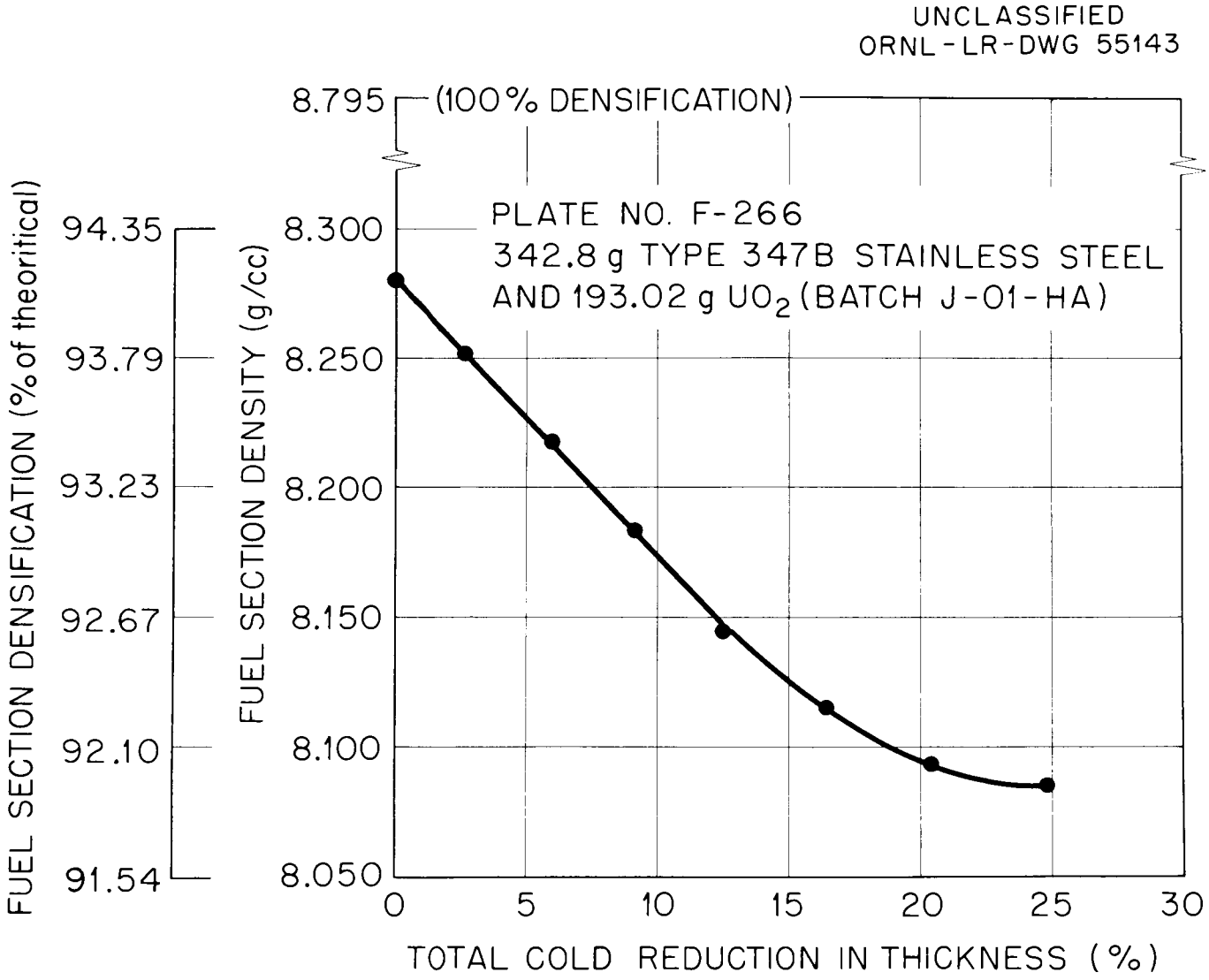

Fig. 13 Effect of Cold Reduction on Densification of UO_2-Stainless Steel Fuel Section.

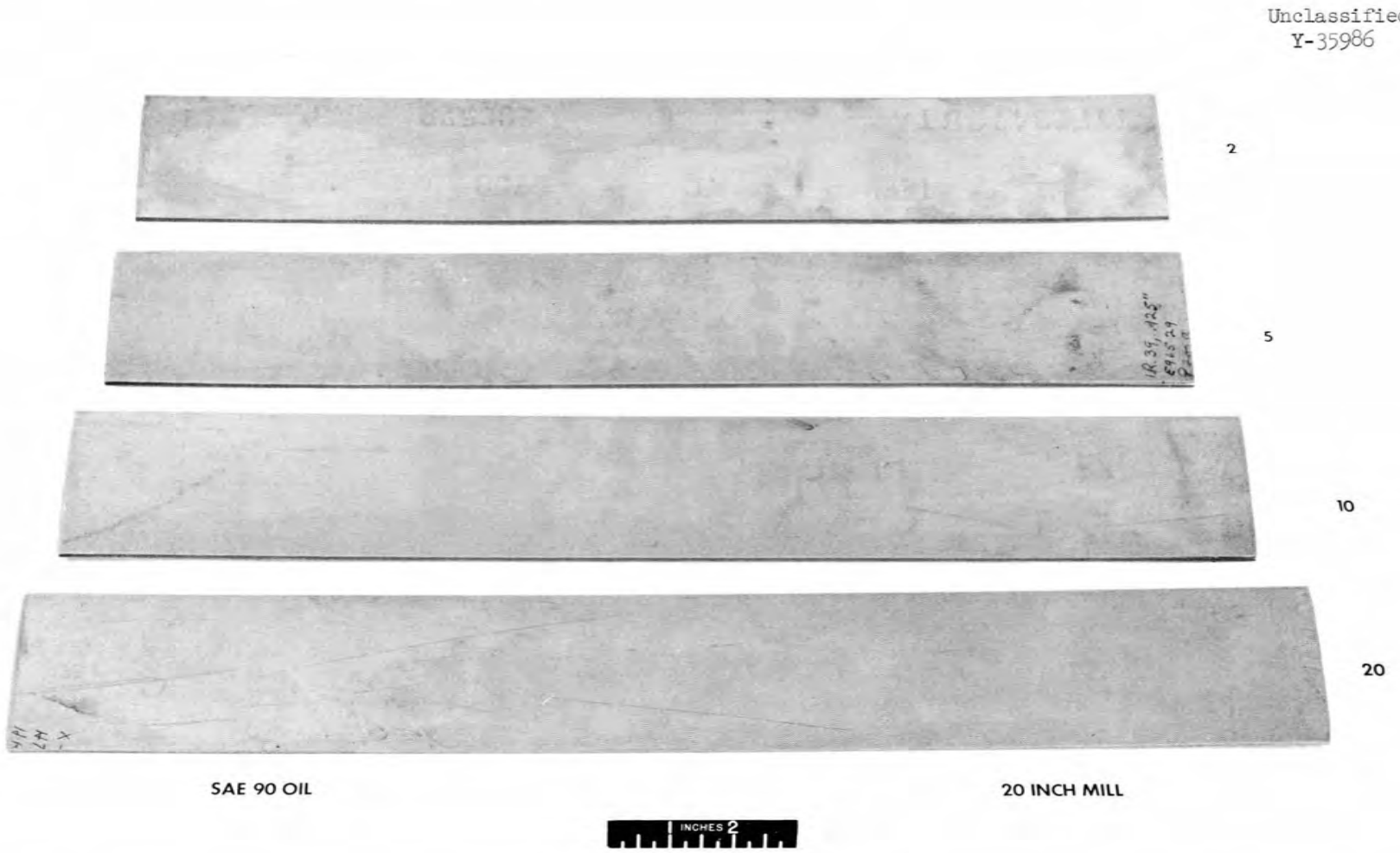

Fig. 14 Comparison of Flatness of Annealed Wrought Type 347 Stainless Steel after Cold Reductions in Thickness from 2 to 20% on the 20-in.-Diam x 30-in.-Face 2-High Mesta Mill. Thickness of plate prior to cold reduction, 0.125 in. Figures at right indicate percent cold reduction.

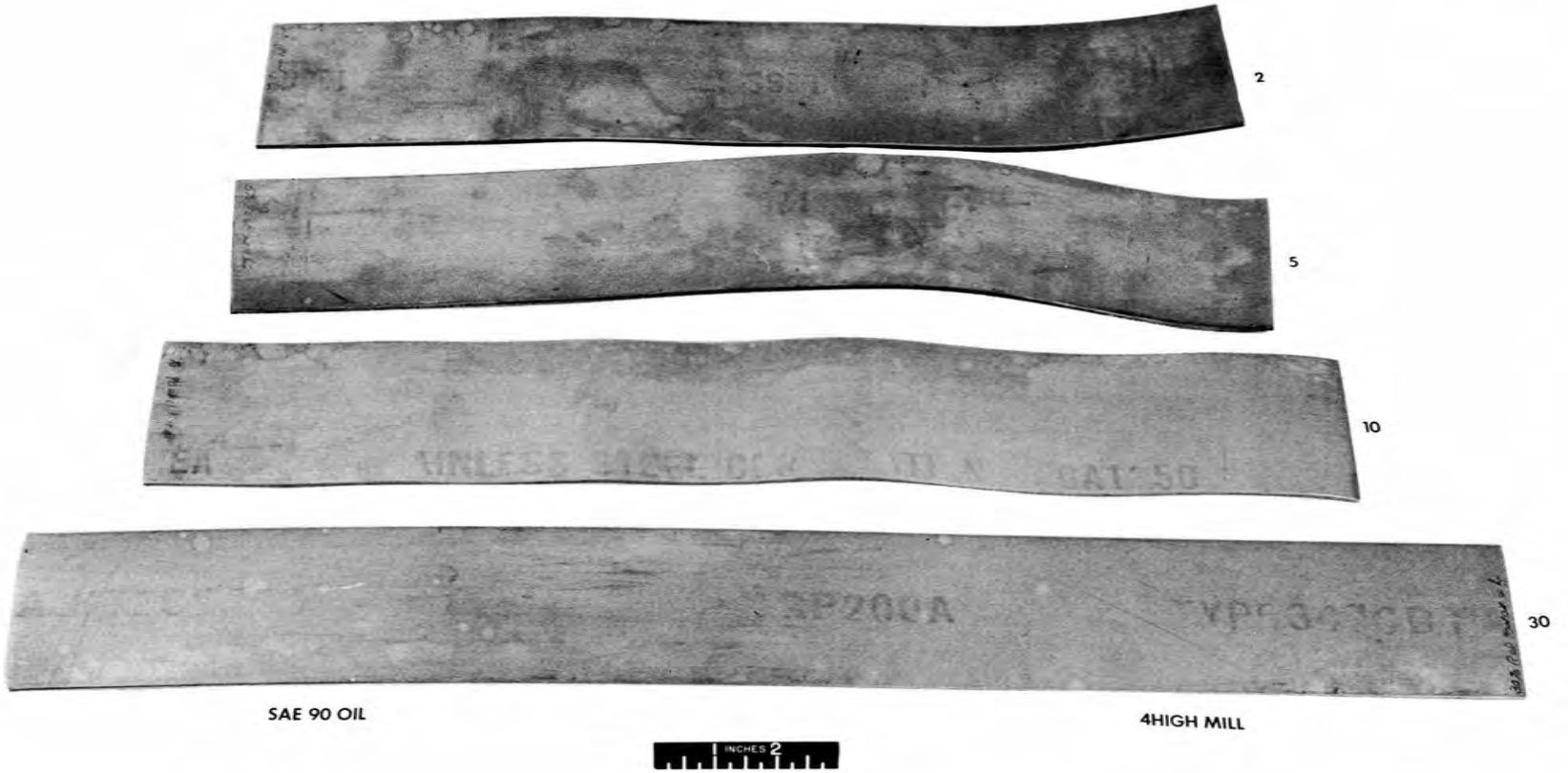

Fig. 15 Comparison of Flatness of Annealed Wrought Type 347 Stainless Steel after Cold Reduction in Thickness from 2 to 20% on the 4-High Bliss Mill. Thickness of plate prior to cold reduction, 0.125 in. Figures at right indicate percent cold reduction.

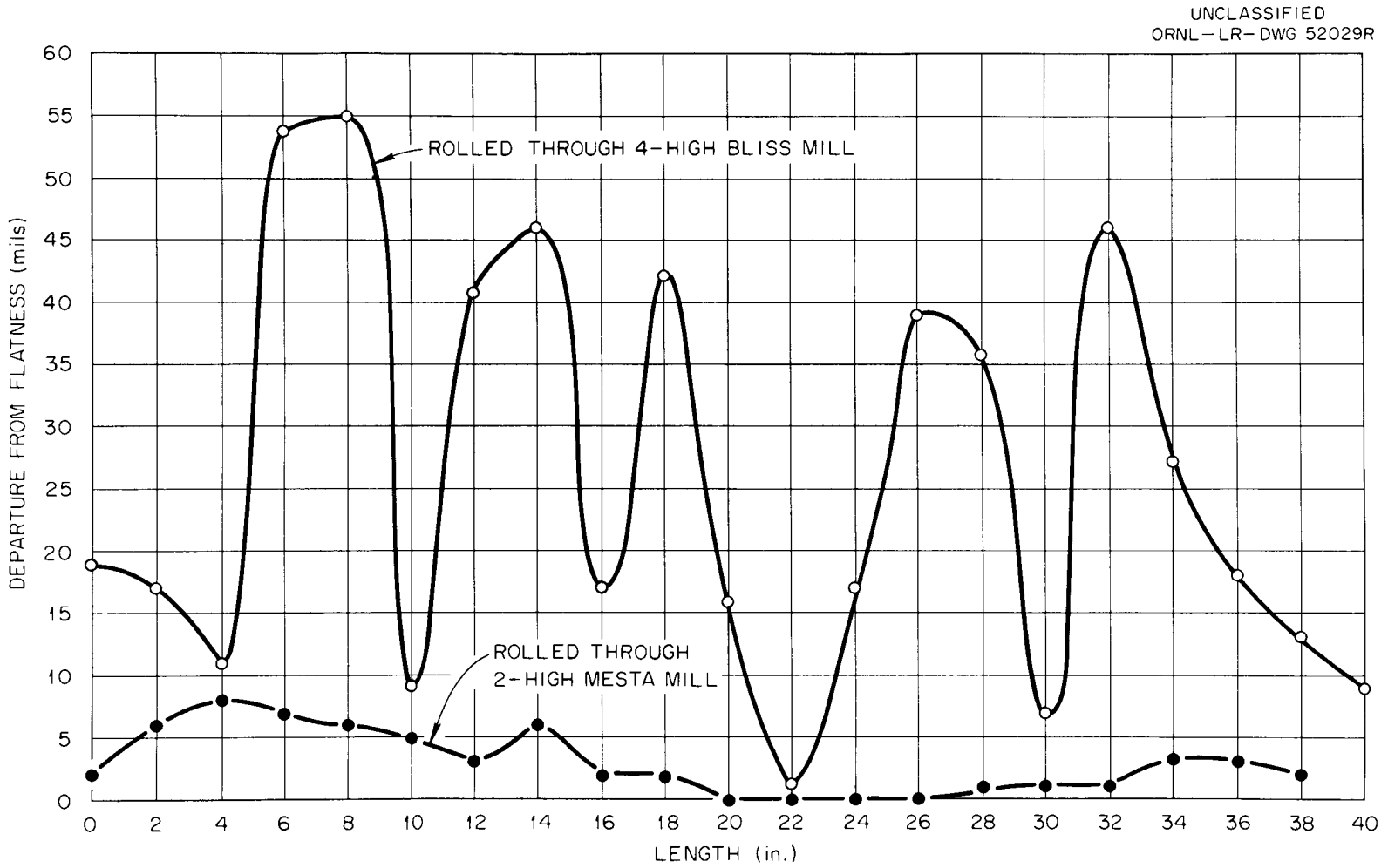

Fig. 16 Comparison of Flatness of Prototype Plates Cold Rolled 3.5% Through the 4-High Bliss Mill and the 2-High Mesta Mill and Flatten Annealed at 1150°C.

FUEL PLATE FABRICATION

Component Design and Fabrication

Although it is economically more desirable to prepare only one fuel compact per plate, limitations of available equipment necessitated use of several smaller cores per plate. Four cores were incorporated in Type I plates and two in Type II plates as shown in Figs. 17 and 18, respectively. In the Type I plates, cores of two different lengths were stacked in such a manner that a continuous core-to-core bond line did not exist through the cermet thickness. Thus, local inhomogeneities were minimized.

Type I frames were machined from wrought stock. As illustrated in Fig. 18, the Type II frame contained two cavities separated by a wrought stainless steel insert which allowed fabrication of two plates simultaneously. These frames were machined from sand cast blanks.

The influence of compacting and coining pressures and the effect of sintering temperature, time, and atmosphere on the quality of the fuel core have been well established in previous investigations.[8] On this basis, pressures of 33 and 43 tsi were selected for pressing the powder blend and coining the sintered compact, respectively. (Die design is shown in Appendix A.) The cores were sintered at 1225°C for 1-1/4 hr in hydrogen with a -60°F inlet dew point.

Types I and II billets were prepared by (1) inserting the core compacts into the frame cavity, (2) tungsten inert gas welding of the cover plates to the frame with filler metal, (3) evacuating at room temperature to less than 1 μ, and (4) final sealing of the evacuated billet by hot forging the evacuation stem. Prior to assembly, cover plates and frames were degreased and the mating surfaces were wire brushed with a stainless steel brush.

Billets were preheated in air at 600°C for 1 hr to minimize distortion of the thin cover plates during subsequent heating to the 1200°C rolling temperature. The preheated billets were immediately transferred to an open mouth muffle located in a high-temperature furnace. At the time of the transfer, the furnace was at 1200°C. The workpiece was heated both prior to rolling and between mill passes in protective atmosphere of hydrogen.

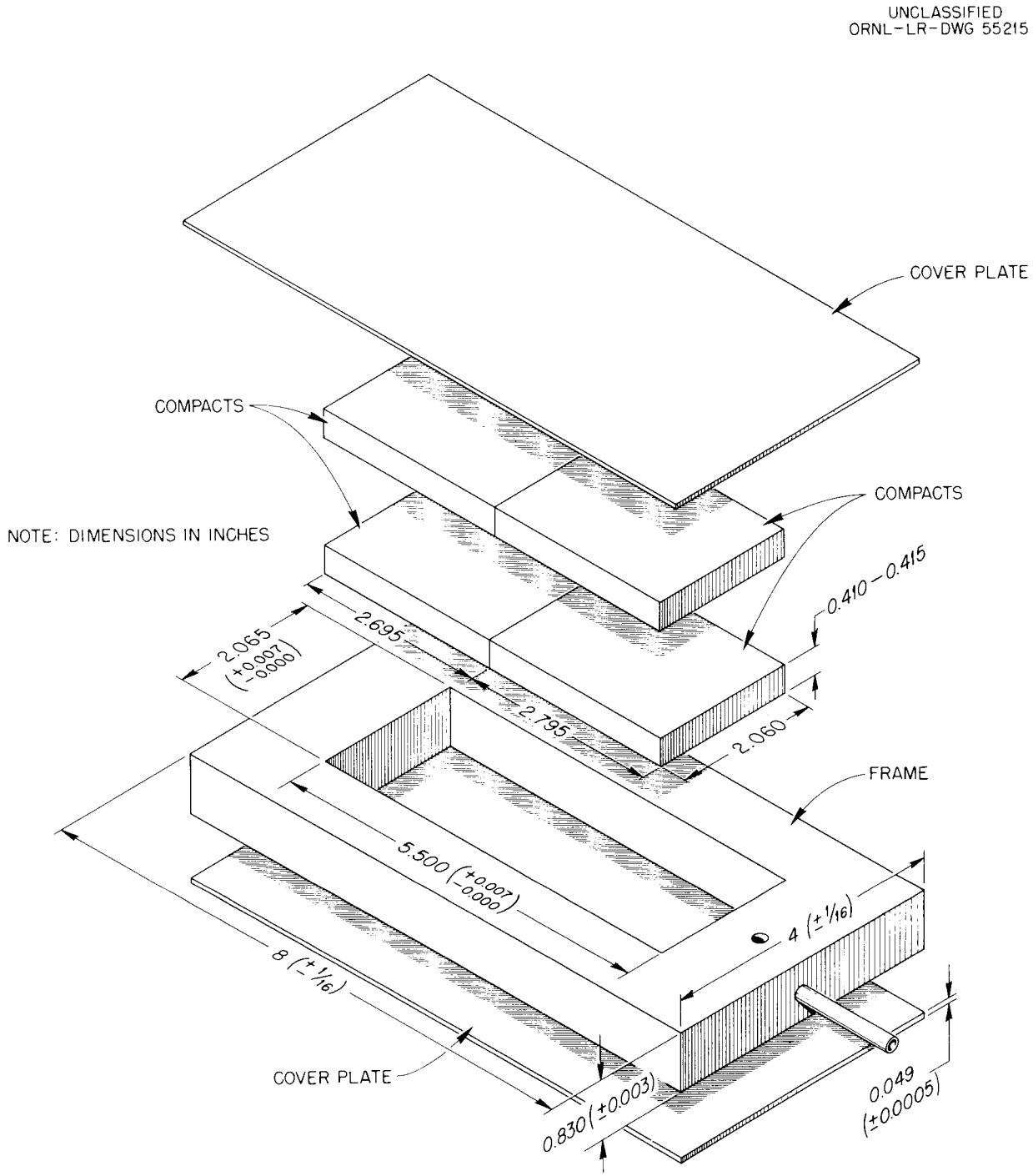

Fig. 17 Type I Fuel Plate Billet Assembly.

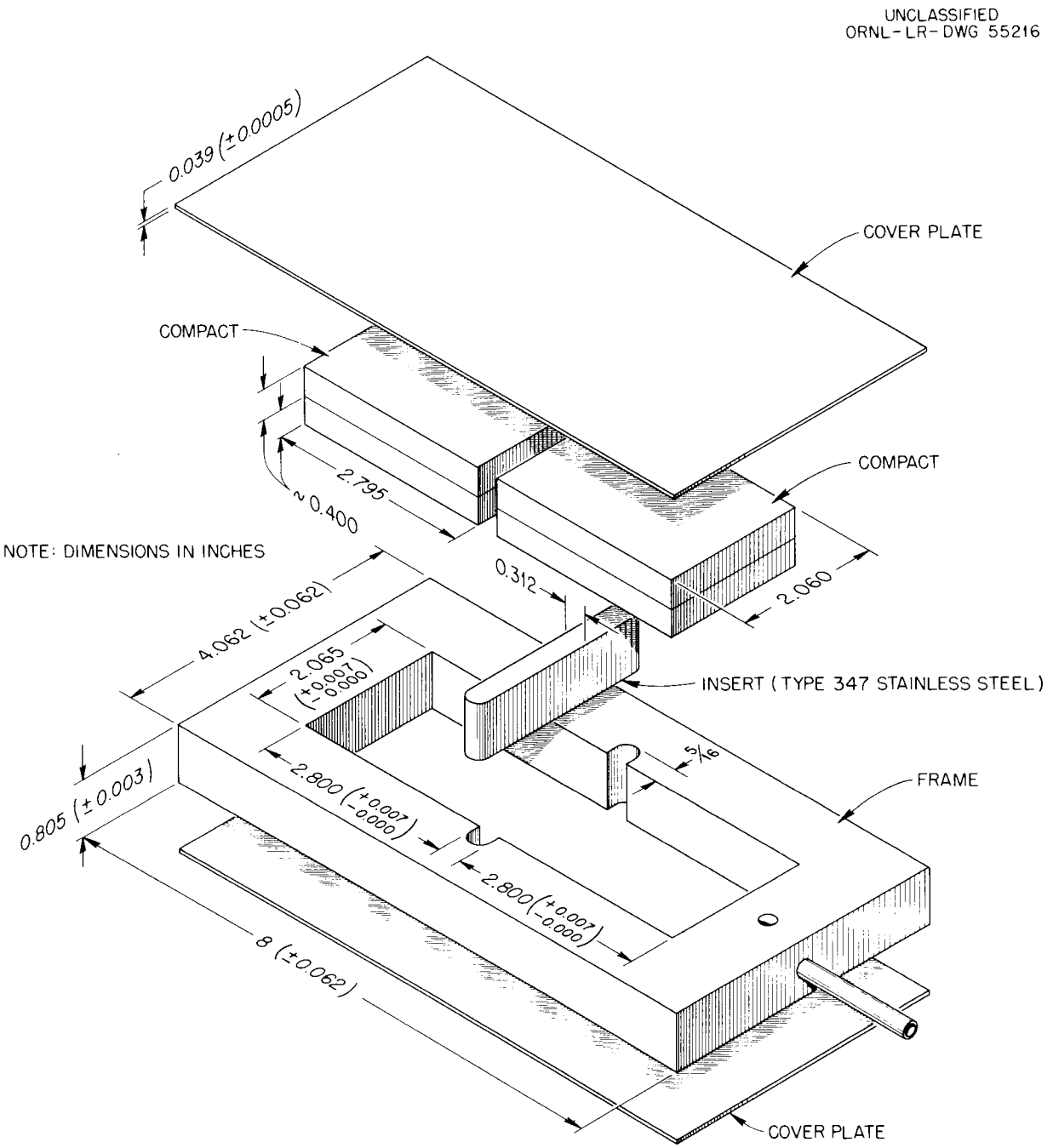

Fig. 18 Type II Fuel Plate Billet Assembly.

A dew point of -30°F was maintained to minimize surface scale formation due to oxidation. Muffle design along with a profile of the temperature gradients along the heated muffle are shown in Fig. 19. Scrupulous attention to cleanliness is essential to good surface quality of fuel plates. Thus, to minimize accumulation of oxide and particulate matter which might mar the surface, all inside surfaces of the muffle were wire brushed daily.

The billets were hot rolled on a 20-in.-diam x 30-in.-face, 2-high Mesta Mill with a reduction per pass schedule, based on mill settings, of two 10% reductions followed by a series of 25% reductions to hot-finished thickness. Between each pass, the plates were rotated 180 deg about their longitudinal and transverse axes. Type I plates were hot rolled to a nominal thickness of 0.116 in. without any cold finishing. Type II plates followed a similar hot-rolling schedule, but were finished by cold rolling to 0.112 in. after the mill scale was removed by pickling in an aqueous solution of 15% HNO_3 and 5% HF.

Prior to establishment of the final size of the billet components, several plates were rolled to define the frame and cover plate dimensions required to produce plates as tentatively specified. Pertinent data summarising these experiments are listed in Tables 5 and 6 for Type I and Type II plates, respectively. The last plate listed in each of these tables is representative of the "production" plates subsequently rolled.

Geometrical Characteristics of Plates

Fuel Section

Several characteristics generally found in composite fuel plates were observed in the UO_2-stainless steel composites fabricated during this program. Three are quite common and were observed while developing similar fuel plates for the SM-1 Reactor. First, the portion of the plate containing the fuel section is thicker, by several mils, than the stainless steel edges and the ends which surround the fuel section. Second, a typical "fishtail" occurs at the end of the fuel section. This effect is illustrated in Fig. 20. Reported length measurements which are based on radiographs include fuel extension due to fishtailing. Third, camber of the fuel core can occur while

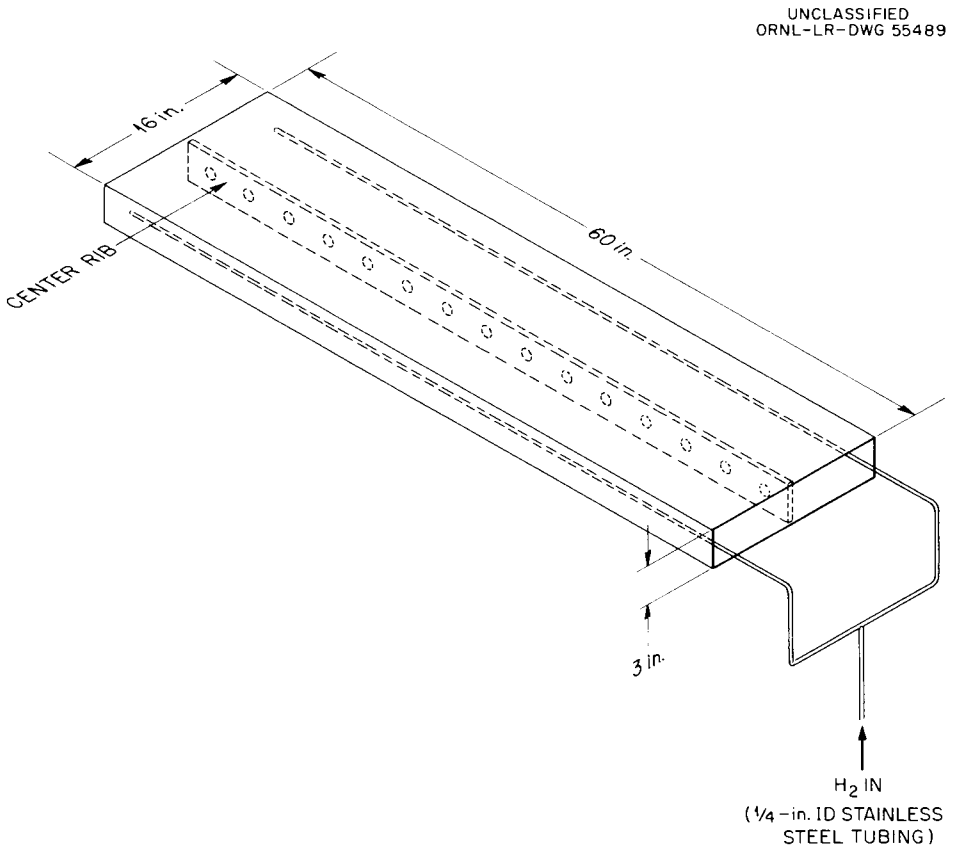

(*a*) MUFFLE DESIGN

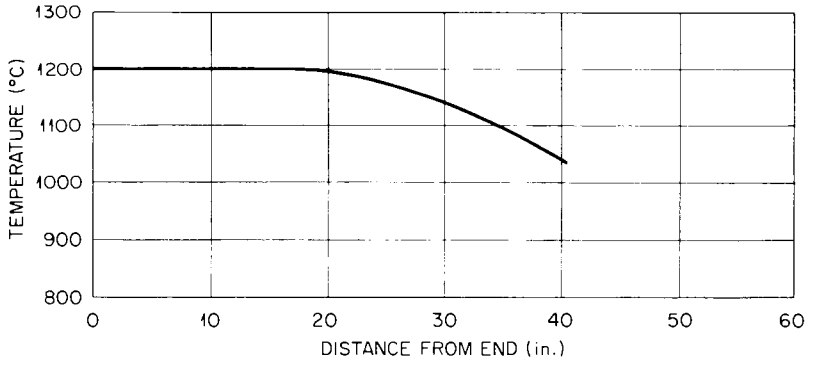

(*b*) TEMPERATURE PROFILE

Fig. 19 (a) Design of Muffle for Preheating Billets, (b) Muffle Temperature Gradients at 1200°C.

TABLE 5

EXPERIMENTAL RESULTS IN ESTABLISHMENT OF FABRICATION REQUIREMENTS FOR TYPE-I PLATES

Plate Number	Frame Thickness (in.)	Cover Plate Thickness (in.)	Frame Cavity		Fuel Concentration		Results				
			Length (in.)	Width (in.)	Stainless Steel (g)	UO_2 (wt %)	Fuel Section (in.) Width max	Fuel Section (in.) Width nominal	Fuel Section (in.) Core Length	Average Clad Thickness (in.)	Nominal Plate Thickness (in.)
F-115	0.846	0.049	5.500	2.070	732.99	33.2	2.156	2.125	36.875	0.007	0.116
F-119	0.837	0.049	5.500	2.065	720.23	33.6	2.156	2.140	36.125	0.007	0.116

TABLE 6

EXPERIMENTAL RESULTS IN ESTABLISHMENT OF FABRICATION REQUIREMENTS FOR TYPE-II PLATES

Plate Number	Frame Thickness* (in.)	Cover Plate Thickness (in.)	Fuel Concentration		Results				
			Stainless Steel (g)	U (wt %)	Fuel Section Dimensions (in.) Core Width max	Core Width nominal	Core Length	Average Clad Thickness (in.)	Modal** Plate Thickness (in.)
170	0.820	0.043	354	35.4	not measured	2.156	18.5	not measured	112
171	0.820	0.043	354	35.4	not measured	2.156	18.5	5.4	112
191	0.780	0.038	339.6	36.2	2.187	2.156	17.80	4.9	112
192	0.780	0.038	339.6	36.2	2.171	2.156	17.89	not measured	112
207	0.805	0.039	342.8	36.0	2.203	2.187	18.00	5.0	113

*Core cavity 2.800 x 2.065 (wide).

**Most frequently occurring value in a series of measurements.

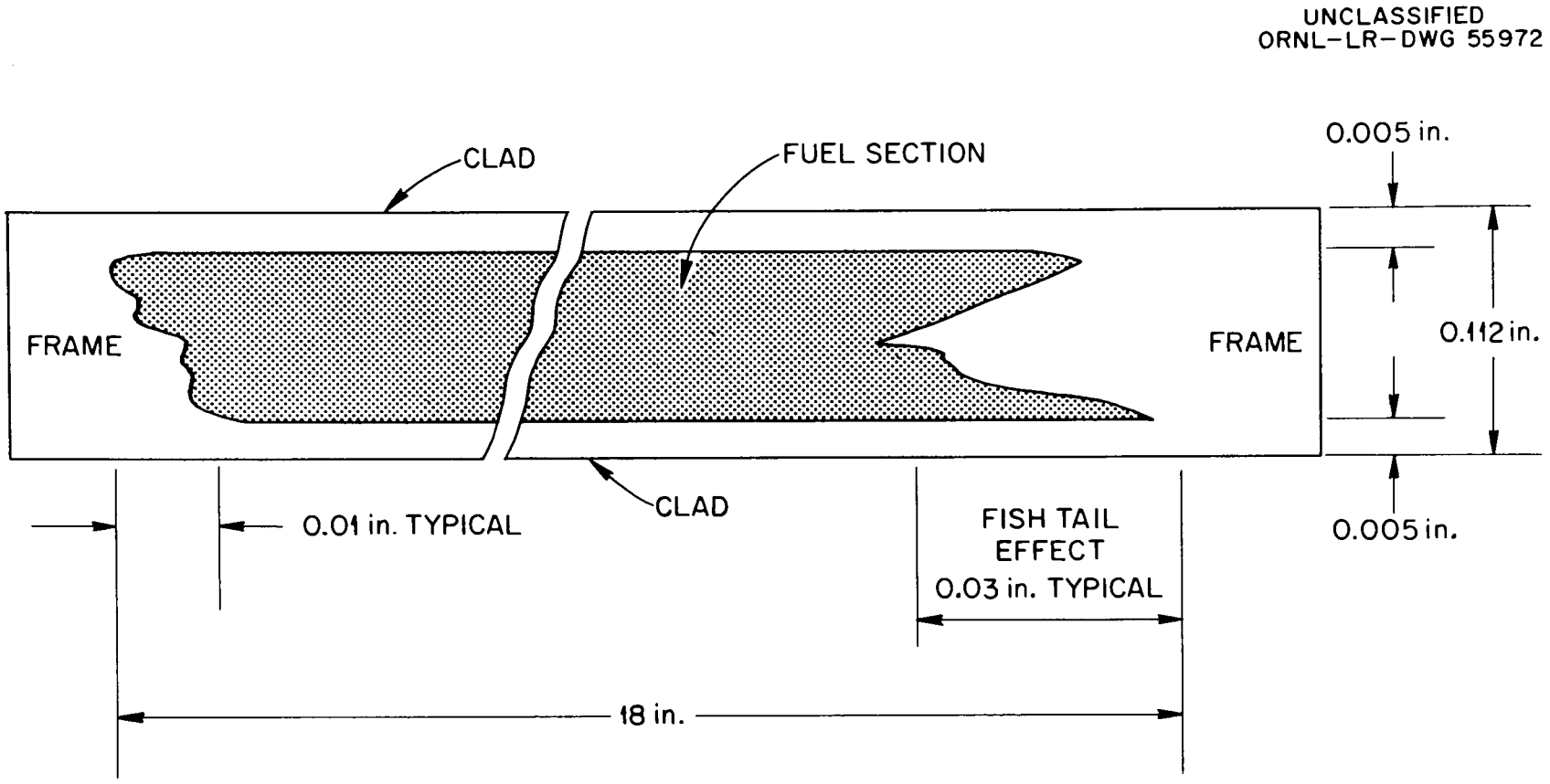

Fig. 20 Typical End Effects in Fermi Core B Composite Fuel Plates.

rolling. This effect is illustrated in Fig. 21. The sagitta is a measure of the magnitude of the camber. It is obvious that as a result of the camber the effective core width is increased.

An effect, which is particularly characteristic of the plates rolled during this program, is flaring of the fuel section width at the ends, as shown in Fig. 22. The consequence of this is a maximum width at the extreme ends of the fuel section, with the nominal width along the balance of the section. To clarify terminology, the nominal width is the width of the fuel core at the midsection; the maximum width is the width at the flared ends and the "effective" width is that measurement which includes the sagitta. In plates with no camber, the maximum width and "effective" width are, of course, identical.

Plate and Clad Thickness

The thickness of the composite plate was measured with a micrometer. Ten random measurements were made along the centerline over the portion of the plate containing the fuel section. The thickness of the stainless steel plate edges and ends was also determined. Cladding thickness was metallographically measured on longitudinal specimens 3/4 in. long removed along the centerline of several test fuel plates. Two of the specimens were taken 2 in. from each end of the core; the other was from the center. Fifteen to twenty random measurements were made on each of these specimens. The cladding thickness is defined as the distance from the surface of the plate to either (1) the bonded stainless steel interface or (2) the nearest surface of the UO_2 particle which may be protruding into the cladding.

Type I "Production" Plates. To establish the reasonableness of the proposed dimensional tolerances and to define an acceptable manufacturing procedure, twenty-eight Type I plates were fabricated by hot rolling at 1200°C with an 87.5% reduction to a final thickness of 0.116. One of the main objectives of the investigation was to determine the feasibility of hot rolling to a finished plate thickness of 0.116 ± 0.003 in. The fuel sections of the first few plates were rolled to lengths greater than 36 in. at the nominal plate thickness of 0.116 in. Rather than adjust the core

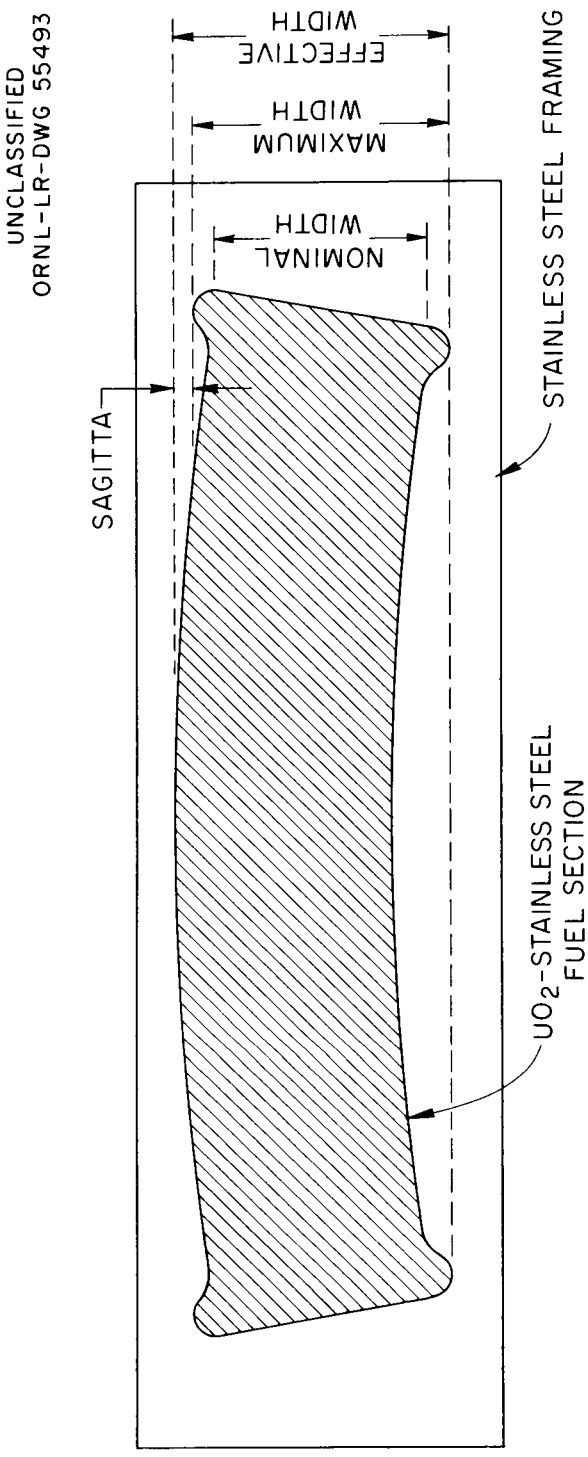

Fig. 21 Plan View Showing Camber of Fuel Section in Composite Fuel Plate.

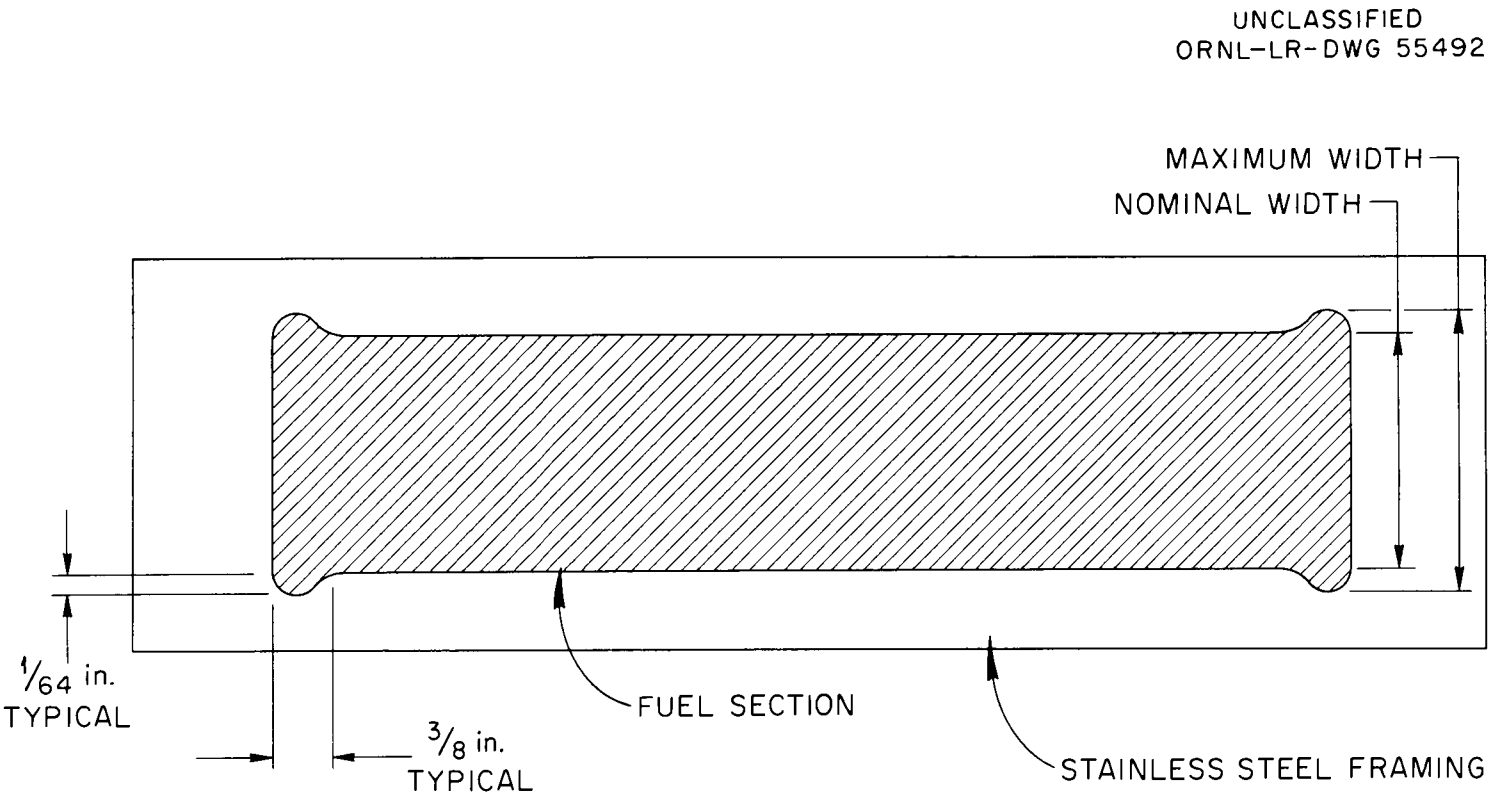

Fig. 22 Plan View Showing "Flaring" Effect at Ends of Fuel Section in Composite Plate.

volume to shorten the length, it was considered expedient to neglect length at this time and obtain performance data on rolling to the 0.116 ± 0.003-in. thickness specification. The pertinent data summarizing the results of dimensional measurements are listed in Table 7 and verify that in 78% of the cases it was possible to hot finish plates to 0.116 ± 0.003 in. Those plates which were not within the thickness specification could have been reheated and rolled to the desired thickness. When plates were reduced to finished thickness by a practice in which the mill setting was changed after each pass, the average variation of plate thickness along its centerline was 1.7 mils. This effect was reduced to 1.1 mils by reducing the plate from 0.120 to 0.116 in. without changing the mill setting. The thickness of the stainless steel edges and ends of plates rolled in this manner is 2 to 4 mils and 4 to 6 mils, respectively, less than the thickness over the fuel section. However, this thickness differential is considerably less immediately adjacent to the fuel section. The results also show that the core length varied from 35.45 to 37.79 in. when the modal or the most frequently occurring measurement of plate thickness ranged between 0.114 and 0.119 in.

Camber in the fuel section of 64% of the plates was observed. The maximum sagitta measured was 0.109 in. Although not investigated, cambering can probably be reduced by employing properly designed guides to assist in feeding the billets through the rolls.

Measurements of the width of the fuel core showed variations along the length, and, as previously illustrated, it was typical for the maximum to occur near the ends of the fuel section. A summary of the nominal width measurements of all plates revealed variations from 2.125 to 2.156 in. The maximum width ranged from 2.156 to 2.204 in.; the "effective" core width ranged from 2.160 to 2.296 in.

In summary, the results revealed that if an application required Type I plates to be hot rolled to 0.116 in. with no additional working to finished size: (1) ±0.003 in. is a reasonable plate thickness tolerance; (2) a fuel section length tolerance of ±0.9 in. is established by (1); and (3) an "effective" core width variation on the order of 0.14 in. would be anticipated.

TABLE 7

SUMMARY DIMENSIONAL DATA OF TYPE I FUEL PLATES

Plate	Core Length Max (in.)	Core Width Max (in.)	Core Width Nominal (in.)	Effective Core Width (in.)	Sagitta (mils)	Thickness of Portion of Plate Containing Fuel Section: Mode (mils)	Maximum (mils)	Minimum (mils)	Total Deviation (mils)
F 141	35.63	2.171	2.125	2.171	0	119.0	119.5	118.0	1.5
F 142	35.63	2.203	2.156	2.251	47	117.0	119.5	116.0	2.5
F 143	35.45	2.187	2.146	2.203	16	117.0	119.5	116.5	3.0
F 144	35.68	2.160	2.125	2.187	27	118.0	119.5	117.5	2.0
F 145	35.77	2.171	2.130	2.171	0	117.0	120.0	120.0	3.0
F 146	35.64	2.171	2.130	2.171	0	118.0	120.0	188.0	2.0
F 147	36.59	2.171	2.130	2.250	79	115.0	117.0	114.0	3.0
F 148	36.75	2.187	2.125	2.281	94	114.5	117.0	114.0	3.0
F 149	36.78	2.171	2.140	2.187	16	115.0	116.5	115.0	1.5
F 150	36.45	2.187	2.140	2.256	69	115.5	116.5	115.0	1.0
F 156	36.38	2.180	2.130	2.160	20	117.0	119.0	116.5	2.5
F 157	36.56	2.160	2.140	2.187	27	116.0	118.5	116.0	2.5
F 158	36.69	2.171	2.140	2.180	9	115.0	117.0	115.0	2.0
F 159	36.75	2.171	2.140	2.187	16	115.0	116.0	114.5	1.5
F 162	36.56	2.160	2.125	2.160	0	116.5	117.0	116.5	1.0
F 173	36.87	2.171	2.130	2.265	94	115.5	115.5	114.5	1.0
F 179	37.28	2.156	2.125	2.156	0	114.0	115.0	113.0	2.0
F 180	37.22	2.171	2.125	2.265	6	115.0	116.5	114.5	2.0
F 181	37.79	2.175	2.130	2.175	0	115.5	117.0	114.0	2.5
F 182	36.89	2.171	2.130	2.286	15	115.5	117.5	115.5	2.0
F 183	36.86	2.203	2.140	2.203	0	114.5	116.0	114.5	1.5
F 184	36.95	2.156	2.140	2.265	109	114.5	116.5	113.5	3.0
F 185	36.60	2.187	2.156	2.296	9	115.5	116.0	115.0	1.0
F 186	36.86	2.171	2.140	2.171	0	116.5	117.0	115.5	1.5
F 187	37.00	2.160	2.125	2.160	0				
F 188	37.03	2.187	2.156	2.203	16				
F 189	37.08	2.180	2.152	2.180	0				
F 190	36.83	2.187	2.156	2.265	78	114.0	116.0	115.0	3.0

Type II "Production" Plates. Fifty-eight Type II plates were fabricated during this part of the program. Twenty-one plates contained batch "A" UO_2 (J-08-EN), a relatively porous oxide, which did not retain integrity when fabricated into composite plates. The balance of the plates contained batch "B" UO_2 (J-01-HA) which had significantly less porosity than batch "A" and which exhibited acceptable fabricability in composite plates. A comparison of these oxides as the dispersoid in hot-rolled fuel plates is made in Fig. 23. The difference in the appearance of the two oxides is striking.

A summary of the results obtained while fabricating these plates is listed in Table 8. Detailed data are included as Appendix B. An average material loss of 0.24 g per fuel core weighing 267.91 g occurred--less than 0.1%. Since the charged materials are weighed to ±0.01 g and since the material is very carefully handled during processing, it is felt that most of the loss is represented by reduction of the oxide on the stainless steel powders during the hydrogen sintering treatment. Some small loss must also be expected in transferring the paste blend from the blending bottle to the pressing die. Final fuel accountability procedures will be devised by APDA on the basis of these data.

Comparative results between plates containing batch "A" UO_2 and plates containing batch "B" UO_2 reveal significant dimensional differences. First, as reflected by the thickness measurement, coined compacts containing batch "A" oxide were 1.5% less dense than those with batch "B" oxide. It is also apparent that a longer fishtailing at the end of the fuel section and a longer fuel section length were characteristic of plates containing the low quality oxide. The width dimension is similarly affected. Consequently, it is quite obvious that the quality of the oxide must be carefully controlled not only to ensure generation of a suitable microstructure but also to ensure that fuel section dimensions be maintained.

The detailed results listed in Appendix B show that of the fifty-eight plates fabricated, 7% would have been rejected for exceeding the "effective" width of 2.246 in. This is based on an estimated accuracy of ±0.016 in. in the measurement. A 2.246-in. width specification automatically must include this consideration; hence, 2.230 in. is the maximum acceptable measurement.

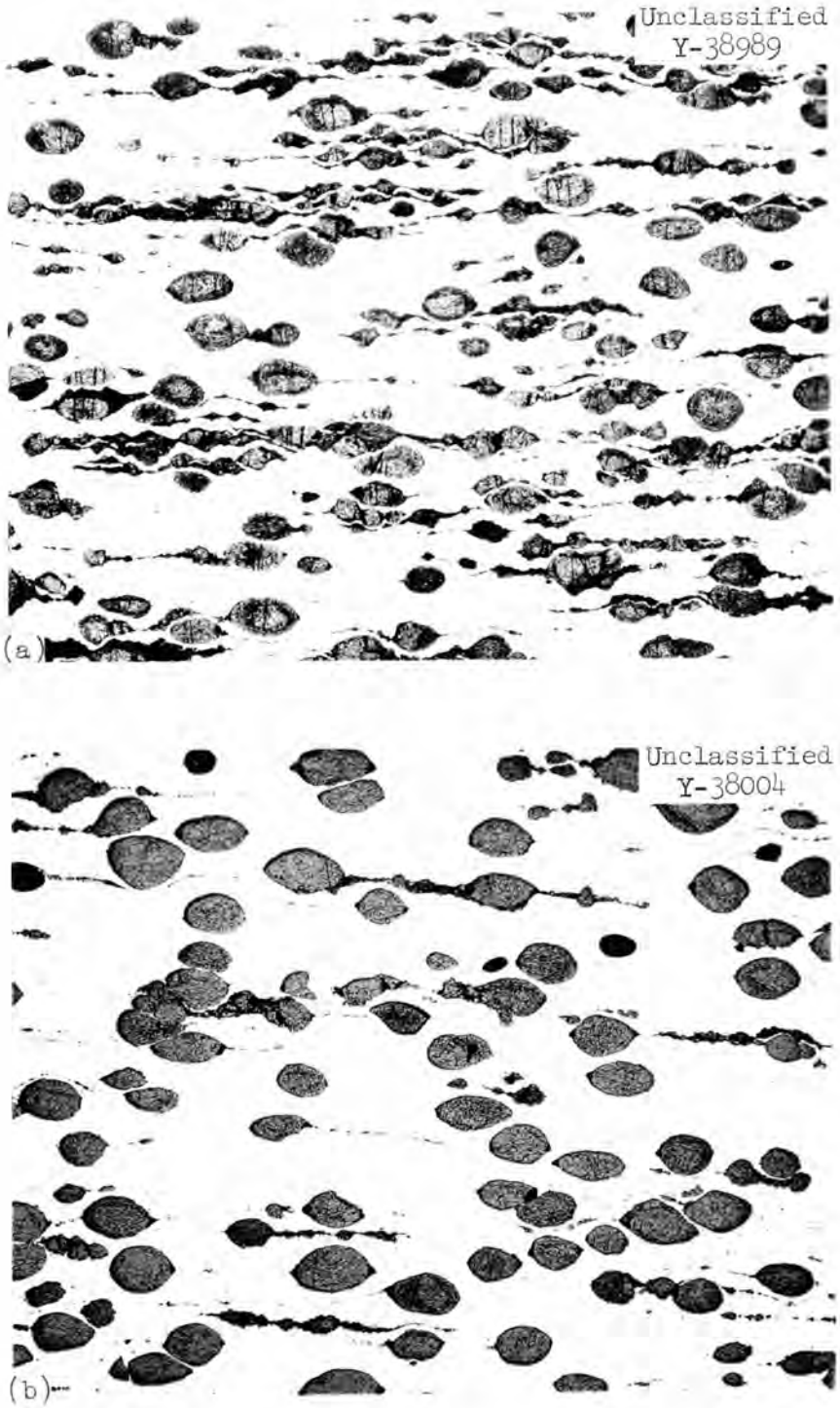

Fig. 23 Comparison Between Poor Quality and Good Quality UO_2 in Fabricated Plate Containing 35 wt % UO_2 in Stainless Steel. (a) Batch A (J-08-EN). Etchant: Aqueous solution of 10% HNO_3-20% H_2O_2. (b) Batch B (J-01-HA). Etchant: Aqueous solution of 10% H_2SO_4-20% H_2O_2. 50X.

TABLE 8

SUMMARY OF DATA ON FABRICATED TYPE II FUEL PLATES

		Average	Standard Deviation*	Range
I.	Weight of Powders (g)	267.91		
II.	Sintered and Coined Fuel Core			
	A. Weight (g)	267.67	± 0.13	267.28/267.90
	B. Thickness (in.)			
	Batch "A"	0.399	± 0.0024	0.392/0.406
	Batch "B"	0.393	± 0.0024	0.385/0.399
	C. Density (g/cc)			
	Batch "A"	7.11 (81.0% of theoretical density)		
	Batch "B"	7.22 (82.2% of theoretical density)		
III.	Fuel Section of Fabricated Plate			
	A. Length (in.)	18.053	± 0.127	17.781/18.297
	Batch "A"	18.168	± 0.094	18.000/18.297
	Batch "B"	17.987	± 0.096	17.781/18.172
	B. Fishtail (in.)			
	Batch "A"	0.309	± 0.098	0.125/0.562
	Batch "B"	0.203	± 0.063	0.125/0.375
	C. Nominal Core Width (in.)			
	Over-all	2.169	± 0.045	2.156/2.203
	Batch "A"	2.181	± 0.007	2.156/2.203
	Batch "B"	2.162	± 0.0024	2.156/2.171
	D. Densification			
	Batch "A"	93.18	± 0.18	92.88/93.56
	Batch "B"	94.39	± 0.26	93.40/94.97

*Standard deviation = $\sqrt{\frac{\Sigma(x-\bar{x})^2}{m-1}}$

where x = individual measurement
$\bar{x}$ = average
m = number of measurements

In addition, it should be noted that the degree of cambering in these plates was appreciably less than the longer Type I plates. The maximum sagitta value was 0.046 in.

All plates were rolled within the ±0.001-in. tolerance on finished plate thickness. In fact, as shown in Fig. 24, 95% of the plates were finished within ±0.0005 in. of their respective modal thickness.

MARKING AND MACHINING PLATES[10]

In order to straddle mill a group of plates to the specified width, two methods were devised for locating the position of the fuel core with relation to the over-all dimensions of the finished composite plate. Both methods are based on the location and transposition of measurements from radiographs to composite plates. Scheme 1 is summarized in Fig. 25 and is self-explanatory. The accuracy of this method is limited by the sheared edge used as a machining reference. Scheme 2, which is illustrated in Fig. 26, offers the advantage that the fuel section centerline is the line of reference. Proportional dividers were used to accurately locate the centerline.

Two different machining jigs were used, each associated with the previously described marking methods. Plates that had been marked in accordance with Scheme 1 were stacked twelve high in the fixture which is illustrated in Appendix C. The sheared reference edges of each plate were aligned by butting them against the side positioning bars. After firmly fixing the plates in position with a hold-down bar, the side positioning bars were removed and the longitudinal edges of the plate straddle milled with the cutters positioned to remove 0.125 in. from the reference edge. Each plate was separately machined to length by end milling one end to the reference mark "E" (Fig. 25). The other end was end milled until the plate was at the specified length dimension.

---

[10] Much of the machining work in this section was performed by R. C. Williams while on loan to ORNL from APDA.

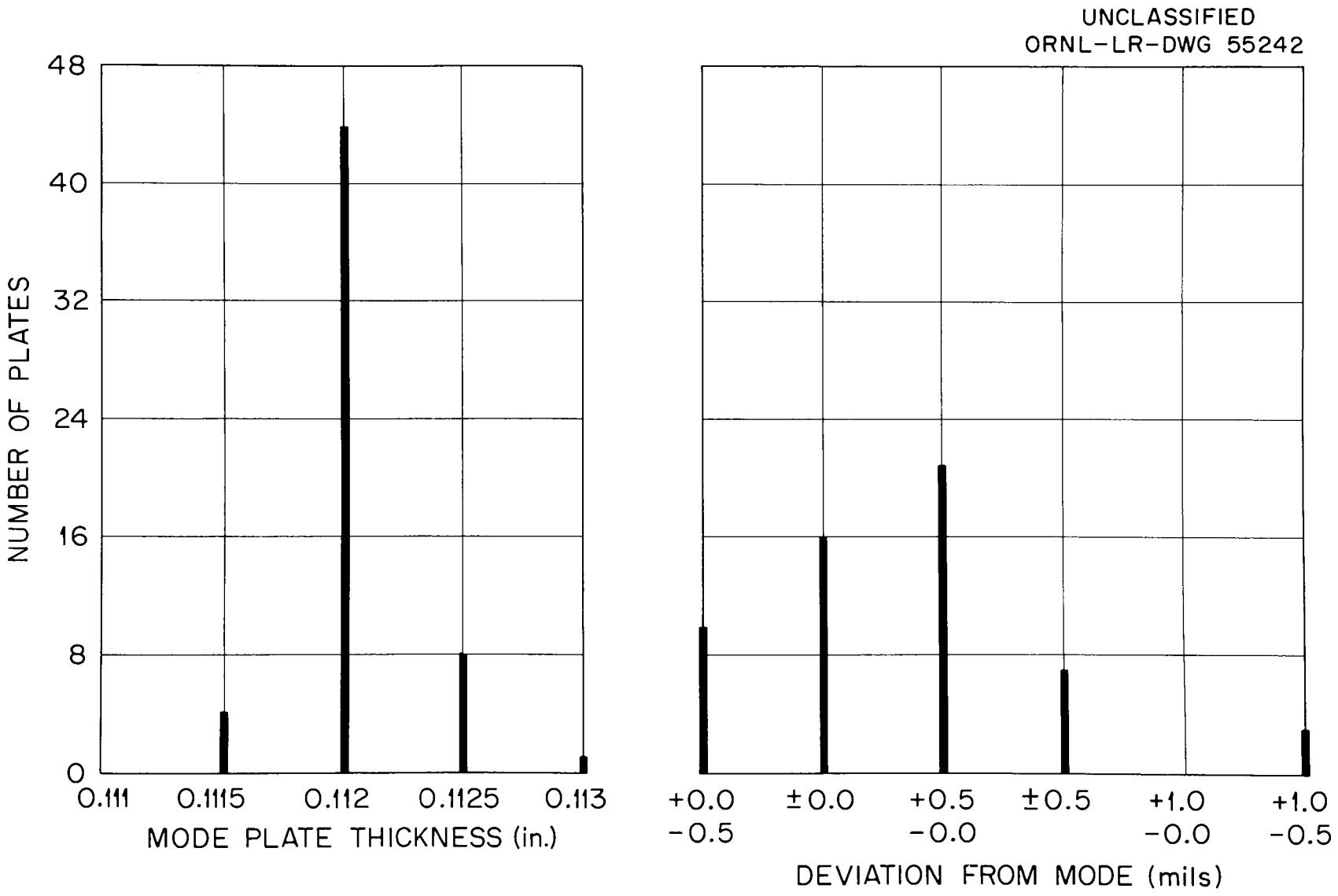

Fig. 24 Summary of the Thickness of the Finished Type II Fuel Plate.

UNCLASSIFIED
ORNL-LR-DWG 55689

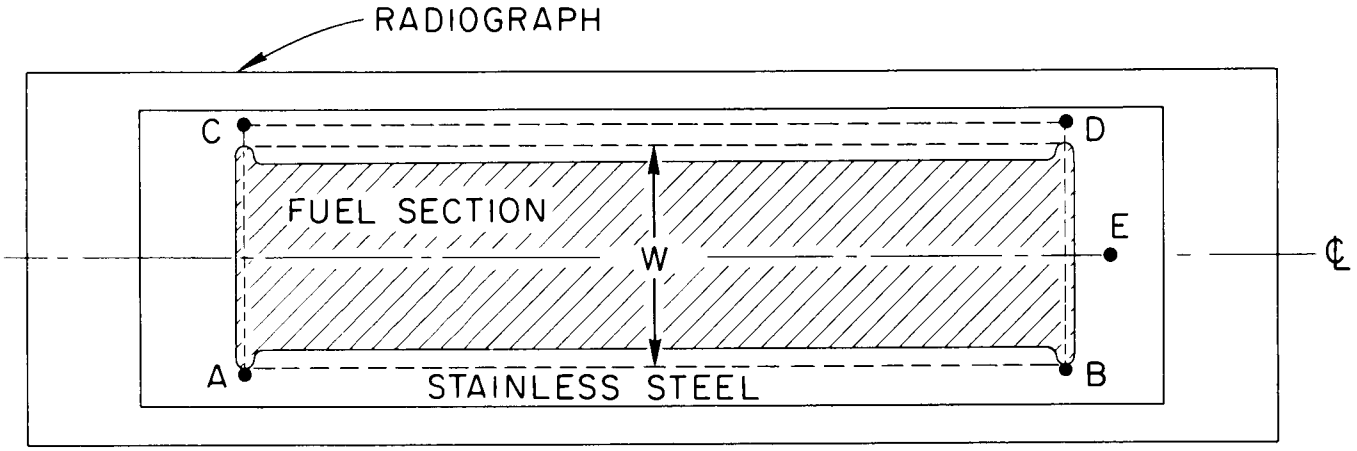

1. MARK ON THE RADIOGRAPH A AND B AND SCRIBE AB
2. DRAW ⊥ TO AB AT A AND B
3. MARK C AND D SO THAT AC = BD = 1.328 in. + $\frac{W}{2}$
   WHERE W = EFFECTIVE CORE WIDTH
4. LOCATE C AND D ON PLATE
5. LOCATE E, $\frac{1}{4}$ in. FROM FUEL SECTION END
6. SHEAR PLATE ALONG CD, THIS IS NOW REFERENCE MACHINING EDGE

Fig. 25 Plate Marking - Scheme 1.

UNCLASSIFIED
ORNL-LR-DWG 55241

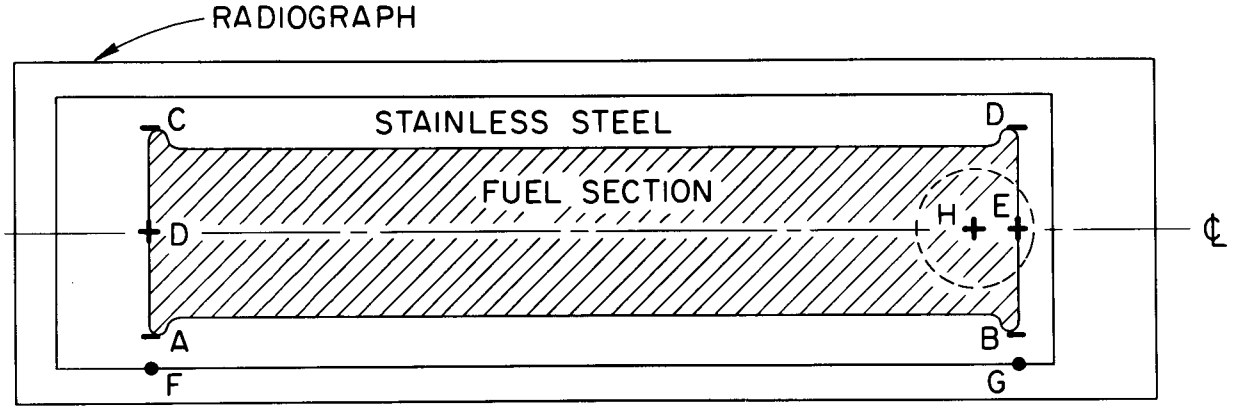

1. MARK D AND E, MID-POINTS OF AC AND BD, ON RADIOGRAPH
2. TRANSFER DF AND EG TO PLATE
3. MARK EXTREME CORE ENDS ON PLATE
4. MARK H, SO THAT HE = $\frac{1}{8}$ in.

Fig. 26 Plate Marking - Scheme 2.

For those plates marked by Scheme 2, machining was initiated by milling the 1/2-in.-diam hole at the extreme end of the fuel section (Fig. 3). The presence of this hole, of course, represents a complicating factor in fuel accountability. This hole and the jig shown in Appendix D were used to position a second locating hole at the opposite plate end on an extension of fuel section centerline. This hole was located in the inactive end of the plate beyond the point where the plate end would be finally established. Twelve plates were threaded through two alignment pins attached to the machining jig, fixed into position with a hold-down bar, and straddle milled. The mid-plane between the milling cutters was coincident with the longitudinal centerline of the machining jig. The ends of the plates were end milled in a stack of twelve. These ends were located using the existing 1/2-in.-diam hole in the fuel section. The other end was machined to the specified plate length.

The Scheme 1 marking process proved unsatisfactory. As shown in Table 9, the maximum displacement of the fuel section centerline from the finished machined plate centerline was 0.105 in. in one of fourteen plates so marked; the average displacement was 0.054 in. In general, the fuel section centerline was not displaced parallel to the plate centerline but at an angle to it.

Two sets of twelve plates each were marked and machined according to the Scheme 2 method. The maximum centerline deviation in one plate of Set B was 0.075 in. and the average was 0.030 in.; in Set C, the maximum was 0.035 in. and the average was 0.024 in. The reduction of both the maximum and average deviations in Set C may be attributed to increased operator experience. These results show that Scheme 2 is superior to Scheme 1 but still results in a displacement of the plate centerline from the fuel section centerline. The displacement must be considered when establishing final tolerances on the width of the fuel section. By employing Scheme 2, the displacement can probably be held to less than 0.030 in. Therefore, the "effective" core width must be maintained at 2.200 in. maximum to ensure the minimum inactive edge of 0.080 in., shown previously in Fig. 3.

No difficulties were experienced in machining the perimeter of the plates. However, initial attempts to drill the 1/2-in.-diam hole in the

TABLE 9

RESULTS OF MARKING METHODS ON FUEL SECTIONS
CENTERLINE IN FINISHED PLATE

Marking Scheme		
1	2	2
Plate Group		
A	B	C
Maximum Divergence of Fuel Centerline From Finished Plate Centerline (in.)		
0.045	0.025	0.025
0.040	0.050	0.015
0.070	0.040	0.030
0.060	0.075	0.035
0.050	0.030	0.035
0.052	0.015	0.020
0.035	0.005	0.015
0.070	0.010	0.030
0.105	0.015	0.025
0.065	0.020	0.000
0.060	0.030	0.035
0.060	0.045	0.025
0.020		
0.025		
Average 0.054	0.030	0.024

fuel plate resulted in an elliptical hole. This was due to the fact that half of the hole was in the stainless steel end and half in the fuel section and the tool wandered during drilling. The condition was remedied by first locating the centerline of the hole with a center drill, drilling with a 1/4-in. drill, and then squaring and reaming the hole with two-fluted end-mill cutters in successive steps of 0.375, 0.475, 0.490, 0.499, and 0.501 in.

FLATTENING FUEL PLATES

During annealing, plates were handled in batches of fourteen which is the number required in the make-up of one fuel bundle. Preannealing treatment consists of degreasing and painting each plate with a suspension of 5% levigated alumina in water. The stack was placed between 1/2-in.-thick platens, the assembly bolted together to facilitate handling, and dried overnight at 150°C. Very light bolting torque is required since the weight of the platens and plates was sufficient to obtain satisfactory flatness. Platen design is shown in Appendix E.

The assembly of plates was placed in a controlled atmosphere muffle furnace at 300°C. Helium gas was used to purge the muffle until a temperature of 650°C was exceeded, at which time hydrogen was introduced into the furnace. The rate of heating to a temperature 1150°C was approx 400°C/hr. After annealing for 2 hr at 1150°C the plates were furnace cooled to 650°C, the muffle purged with helium, and the plates removed from the muffle at 300°C. After removal from the platens the plates were washed in water to eradicate all traces of alumina.

SURFACE FINISH

Surface quality of UO_2-bearing plates was evaluated by measurement of the average surface roughness as well as the distribution and depth of pits. Surface roughness of Type II plates varied between 20–40 μin. (rms) as determined by a surface profilemeter.

A pit depth-frequency chart for fifty-eight Type II plates is illustrated in Fig. 27. Pit depth was determined with a Zeiss Light Section Microscope.

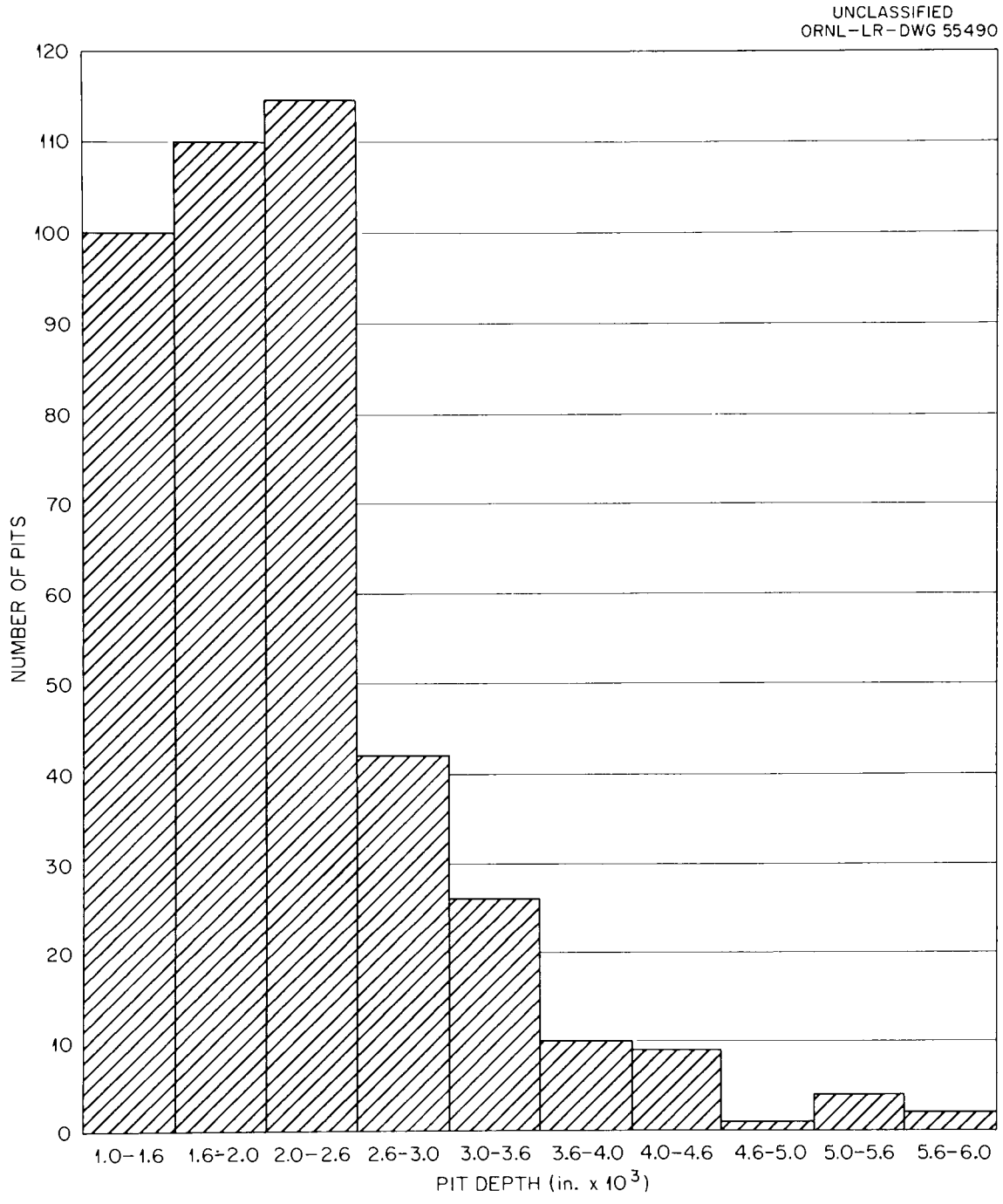

Fig. 27 Pit Depth-Frequency Distribution in Surfaces of Cold Rolled Type II Plates.

It may be noted that 12% of the total number of pits deeper than 0.001 in. exceeds the specified minimum cladding thickness of 0.003 in.; whereas, less than 1% exceeds 0.005 in., the nominal thickness. Based on the observed pit distribution, the probability of any pit penetrating into a UO_2 particle is less than 1/2% at a nominal clad thickness of 0.005 in. Detailed probability calculations are listed in Appendix F.

The frequency of pits deeper than 0.002 in. was somewhat surprising in view of the care exercised in maintaining cleanliness in the muffle of the preheat furnace, the rolls, and roll table of the mill. It is to be pointed out that the general practice during preheating was to lay the billets horizontally in the muffle. An improvement might be expected if the billets were placed vertically. Any oxide which would form on the surfaces might then spall off.

The pitting data were alternately evaluated to determine a basis for plate rejection due to pit depth. Figure 28 is a plot of rejection frequency vs maximum specified pit depth based on the fifty-eight Type II plates. This analysis shows that if a specification calls for rejection of a plate with a pit depth of 0.002 in. or greater, 100% rejections would have occurred. Likewise, if the acceptance standard on pit depth was set at 0.003 in., 95% would be in the rejection category. In fact, even with a specification allowing pits as deep as the nominal cladding thickness itself, 15% of the plates would have been rejected. These results point up the need for scrupulous care in the processing of fuel plates to avoid pitting due to scale formation and embedment in the surface during hot working. A final specification on quantity and magnitude of pitting awaits analysis by the APDA design group.

CONCLUSIONS

1. Homogeneous dispersions of 35 wt % spheroidal UO_2 in stainless steel can be prepared by employing a wetting agent of 5% paraffin in CCl_4 to prevent classification of the powder mixture during blending and subsequent handling operations. The resulting standard deviation of uranium concentration from point to point within a composite plate prepared in this manner is less than ±0.15 wt %.

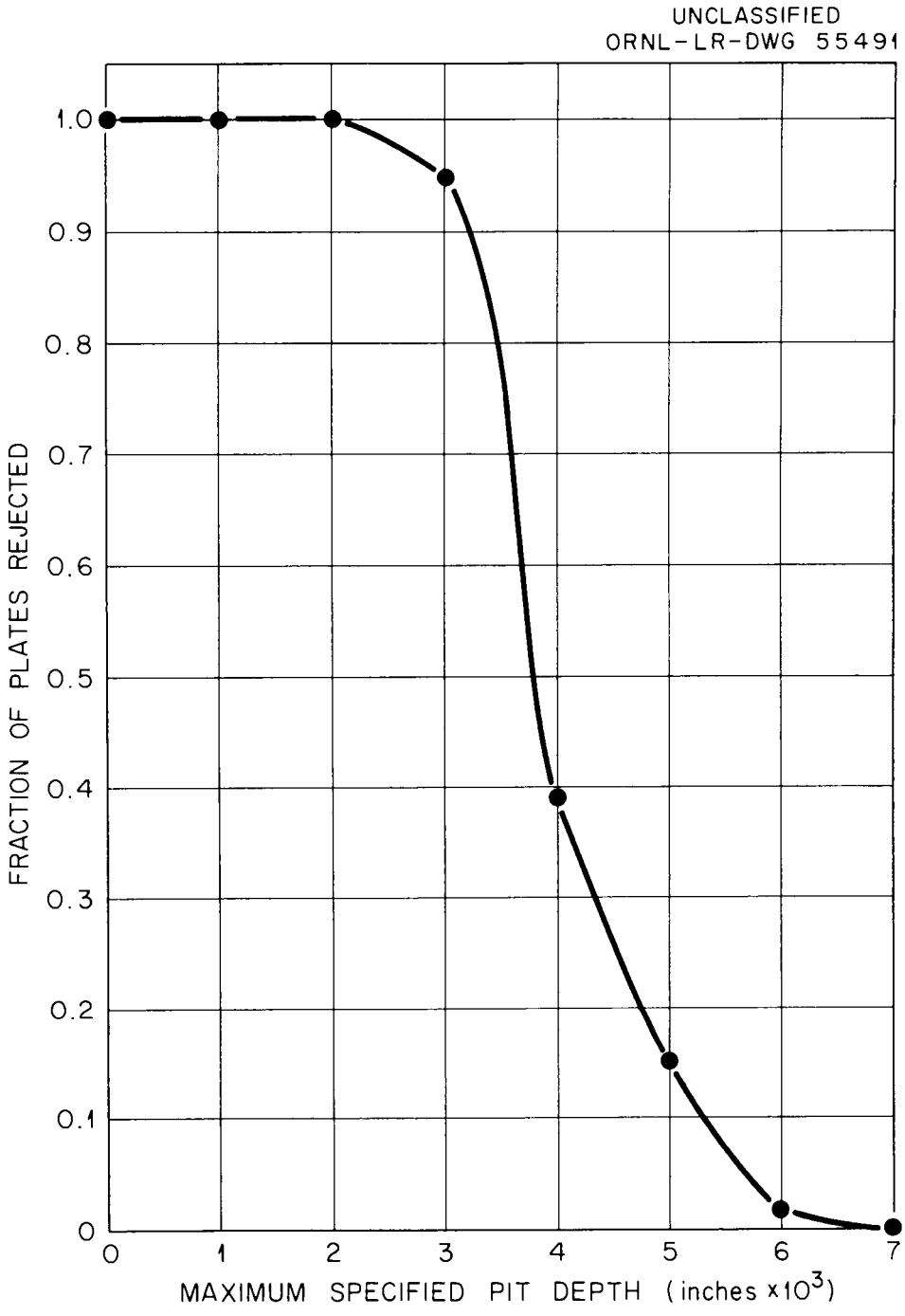

Fig. 28 Relationship Between Specified Maximum Pit Depths and Plate Rejections Based on Experience in Fabricating Fifty-Eight Type II Fuel Plates.

2. A density of 81% of theoretical can be achieved in compacts 2.1 in. x 2.8 in. x 0.4 in. by room-temperature pressing at 33 tsi, sintering for 1-1/4 hr in dry hydrogen at 1225°C, and room-temperature coining at 43 tsi.

3. Satisfactory bonding of type 347 stainless steel cladding to the type 347 stainless steel frame and the 35 wt % UO_2–type 347 stainless steel fuel compact can be attained by roll cladding at 1200°C with a total reduction in thickness of 87.5%.

4. The structural integrity of spheroidal UO_2 appears to depend primarily upon the internal structure and the bulk density of the particles prior to plate fabrication.

5. Fuel sections in which the UO_2 retains its spheroidal structure have higher densities than those containing UO_2 of poor fabricability.

6. Fragmentation and stringering of the high quality spheroidal UO_2 dispersed in the composite plate is not excessive at cold reductions in thickness of less than 10%.

7. Density of the fuel section is inversely proportional to cold reduction in thickness within the range of 0 to 20%.

8. Acceptable flatness of the plates can be maintained when cold rolled on a 20-in.-diam 2-high rolling mill, using SAE 90 oil as a lubricant.

9. The surface finish of plates cold reduced 3.5% in thickness is in the range of 20–40 μin. (rms).

10. A problem which may be encountered in full-scale manufacturing is pitting of the surfaces of the composite fuel plates.

11. The effective fuel section width is increased because of inaccuracies in plate marking for final machining.

12. The dimensions of the Core B composite plate can be maintained to rigid tolerances in a roll-cladding process.

13. An outline of the fabrication procedures which will result in satisfactory Type II composite fuel plates is given in Appendix G.

ACKNOWLEDGMENTS

The authors are indebted to R. C. Williams, of APDA, who established the bulk of the fuel plate machining practices.

Additionally, thanks are extended to A. L. Lotts and S. A. Rabin of the Powder Metallurgy Group for their assistance in preparation of the fuel cores; C. K. H. DuBose and J. A. Lockett of the Metallography Group for their cooperation; W. C. Colwell of Graphic Arts for assistance in illustrating this document; and to Geneva Harris and Susan Thompson of the Metallurgy Reports Office for their patient service in typing the report. Recognition is also afforded M. M. Goff, Mathematics Panel; A. B. Keeney, Machine Shop; R. W. Laing, Chemistry; and to E. R. Turnbill and the other technicians of the Fuel Fabrication Group. The coordination and suggestions of W. C. Thurber of the Project Metallurgy Group and A. A. Shoudy of APDA were of great value and their efforts are appreciated.

APPENDIX A

POWDER METALLURGY DIE DESIGN

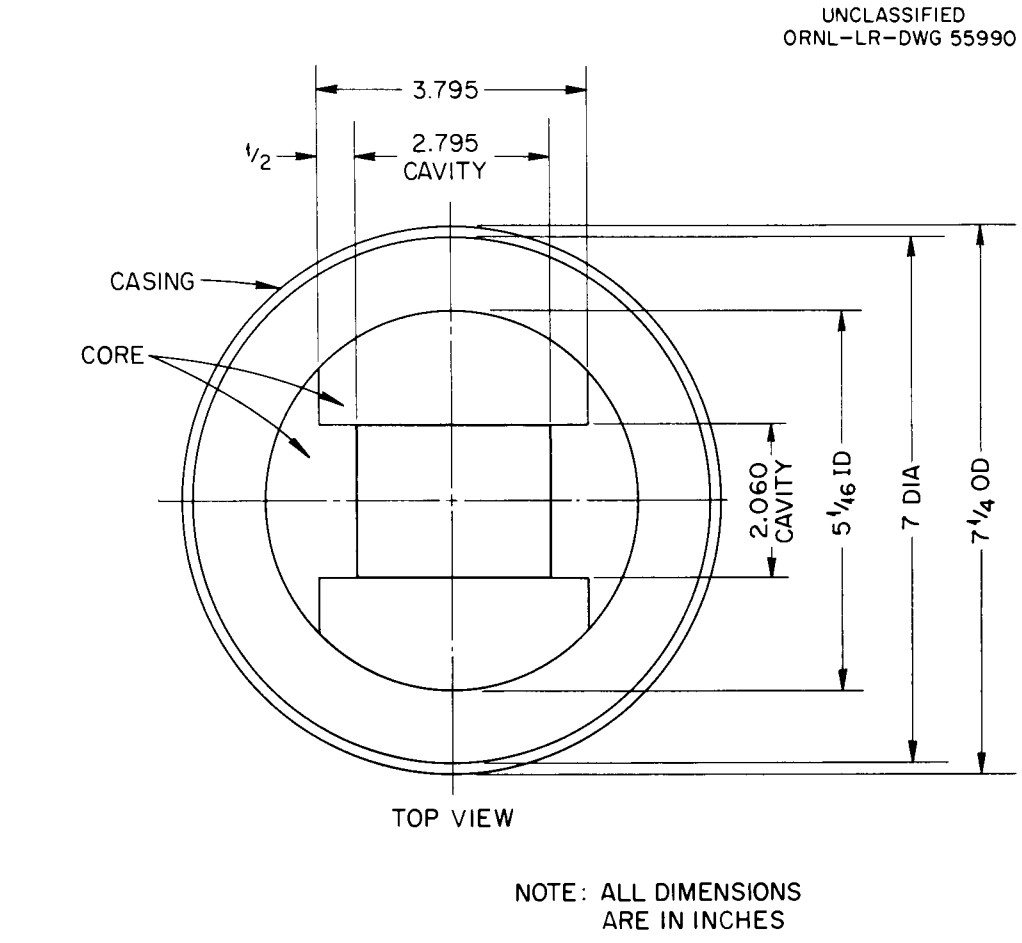

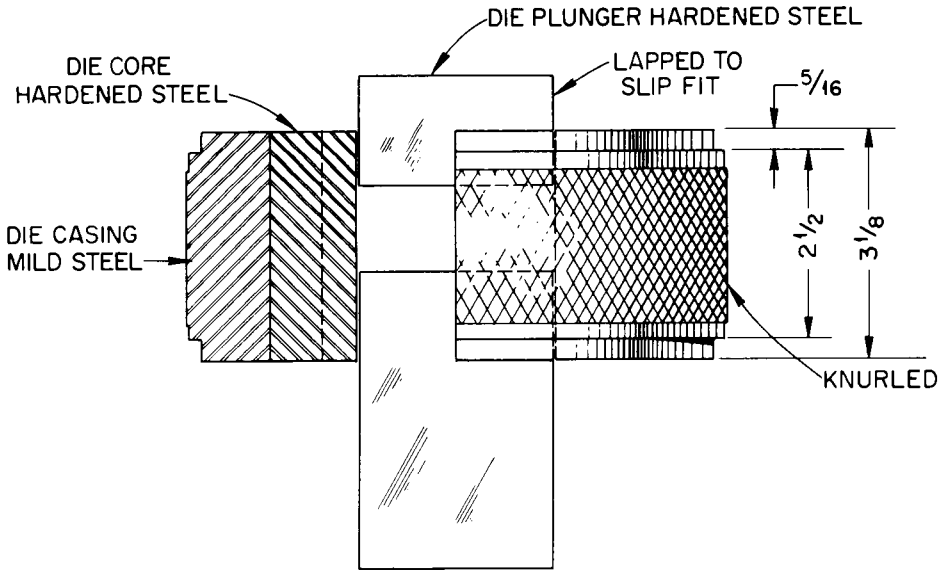

Fig. 29 Powder Metallurgy Die Design.

APPENDIX B

SUMMARY OF PERTINENT DIMENSIONS FOR 18-IN.-LONG CORE B PROTOTYPE PLATES

SUMMARY OF PERTINENT DIMENSIONS FOR 18-IN.-LONG CORE B PROTOTYPE PLATES[a]

Plate Number[b]	Core Specifications					Plate Thickness Including Fuel Section		
	Maximum Core Length[c] (in.)	Total Flashover (in.)	Nominal Core Width[d] (in.)	Maximum Core Width (in.)	Maximum Effective Core Width[e] (in.)	Mode[f] (mil)	Deviation From Mode	
							− (mil)	+ (mil)
F 193	18.281	0.375	2.156	2.156	2.156	112	0.5	0
F 194	18.031	0.406	2.156	2.218	2.218	112.5	0	0.5
F 195	18.109	0.281	2.187	2.203	2.203	112.5	0	0.5
F 196	18.062	0.250	2.203	2.203	2.218	112	0	0
F 197	18.187	0.375	2.171	2.187	2.187	112	0	0.5
F 198	18.297	0.562	2.187	2.218	2.218	112	0	0
F 199	18.204	0.312	2.171	2.203	2.249	112	0	0
F 200	18.266	0.187	2.171	2.203	2.249	112	0	0
F 201	18.111	0.562	2.187	2.203	2.213	112.5	0	0
F 202	18.234	0.250	2.187	2.203	2.203	112.5	0	0.5
F 203	18.078	0.375	2.187	2.194	2.209	112.5	0	0
F 204	18.297	0.312	2.187	2.203	2.225	112	0	0
F 205	18.047	0.187	2.179	2.187	2.187	112.5	0	0
F 206	18.234	0.375	2.196	2.196	2.232	112	0	0.5
F 207	18.000	0.250	2.187	2.203	2.234	113	0.5	0
F 208	18.156	0.156	2.187	2.218	2.218	112	0	0.5
F 209	18.281	0.250	2.187	2.203	2.203	112	0	0
F 210	18.109	0.125	2.179	2.203	2.203	112	0	0.5
F 211	18.109	0.187	2.178	2.203	2.213	112.5	0.5	0
F 212	18.172	0.187	2.187	2.203	2.203	112	0	0.5
F 213	18.266	0.531	2.171	2.187	2.187	112	0.5	0.5
F 214	18.017	0.218	2.156	2.171	2.171	112	0	0.5
F 215	18.000	0.187	2.171	2.180	2.180	112	0.5	0
F 216	18.125	0.187	2.156	2.171	2.171	111.5	0	0.5
F 217	17.938	0.125	2.156	2.171	2.171	112	0.5	1
F 218	18.063	0.187	2.156	2.171	2.171	111.5	0	0.5
F 219	18.000	0.125	2.165	2.187	2.187	112	0.5	0
F 220	18.063	0.187	2.156	2.160	2.160	111.5	0	0.5
F 221	18.048	0.250	2.156	2.171	2.171	112	0.5	1
F 222	18.041	0.187	2.156	2.171	2.171	112	0	0
F 223	17.906	0.187	2.171	2.187	2.187	112	0.5	0
F 224	17.781	0.187	2.171	2.187	2.187	112.5	0.5	0.5
F 225	17.875	0.187	2.171	2.171	2.171	112	0.5	0.5
F 226	17.922	0.375	2.171	2.187	2.187	112	0.5	0.5
F 227	17.953	0.312	2.156	2.187	2.187	112	0.5	0.5
F 228	18.172	0.281	2.171	2.187	2.202	112	0.5	0
F 229	17.875	0.156	2.156	2.171	2.171	112	0.5	0
F 230	18.062	0.250	2.156	2.187	2.187	112	0	0
F 231	17.875	0.187	2.160	2.171	2.171	112	0.5	0.5
F 232	18.125	0.187	2.156	2.187	2.187	112	0.5	0

SUMMARY OF PERTINENT DIMENSIONS FOR 18-IN.-LONG CORE B PROTOTYPE PLATES[a]
(Continued)

Plate Number[b]	Core Specifications					Plate Thickness Including Fuel Section		
	Maximum Core Length[c] (in.)	Total Flashover (in.)	Nominal Core Width[d] (in.)	Maximum Core Width (in.)	Maximum Effective Core Width[e] (in.)	Mode[f] (mil)	Deviation From Mode − (mil)	Deviation From Mode + (mil)
F 233	17.968	0.125	2.171	2.171	2.171	112	0.5	1
F 234	18.000	0.125	2.171	2.171	2.171	112	0	0.5
F 235	17.906	0.250	2.171	2.187	2.187	112	0.5	0.5
F 236	17.781	0.125	2.171	2.203	2.203	112	0	0.5
F 237	17.969	0.187	2.171	2.187	2.202	111.5	0	0.5
F 238	17.953	0.375	2.171	2.180	2.195	112	0.5	0.5
F 239	17.985	0.187	2.171	2.171	2.186	112	0	0.5
F 240	18.141	0.187	2.156	2.187	2.218	112	0	0
F 241	18.000	0.250	2.160	2.187	2.187	112	0	0
F 242	18.125	0.187	2.156	2.187	2.187	112	0	0
F 243	18.000	0.187	2.160	2.171	2.186	112	0	0
F 244	18.041	0.187	2.156	2.187	2.187	112	0	0.5
F 245	17.922	0.312	2.156	2.176	2.176	112	0.5	0
F 246	18.016	0.218	2.156	2.171	2.171	112	0	0.5
F 247	17.906	0.250	2.156	2.187	2.187	112	0	0.5
F 248	18.000	0.125	2.156	2.187	2.187	112	0	0.5
F 249	17.906	0.187	2.171	2.171	2.171	112	0	0.5
F 250	18.063	0.125	2.160	2.187	2.202	112	0	0

[a] All 58 plates used cast picture frames.

[b] Plates F 193 through F 213 contain UO_2 from Batch J-08-EN.
Plates F 214 through F 250 contain UO_2 from Batch J-01-HA.

[c] Includes flashover.

[d] Essentially same as minimum and is measured at midlength.

[e] Includes rainbow.

[f] Eight to nine measurements over core area.

APPENDIX C

MACHINING JIGS APPLICABLE FOR STRADDLE MILLING PLATES MARKED ACCORDING TO SCHEME 1

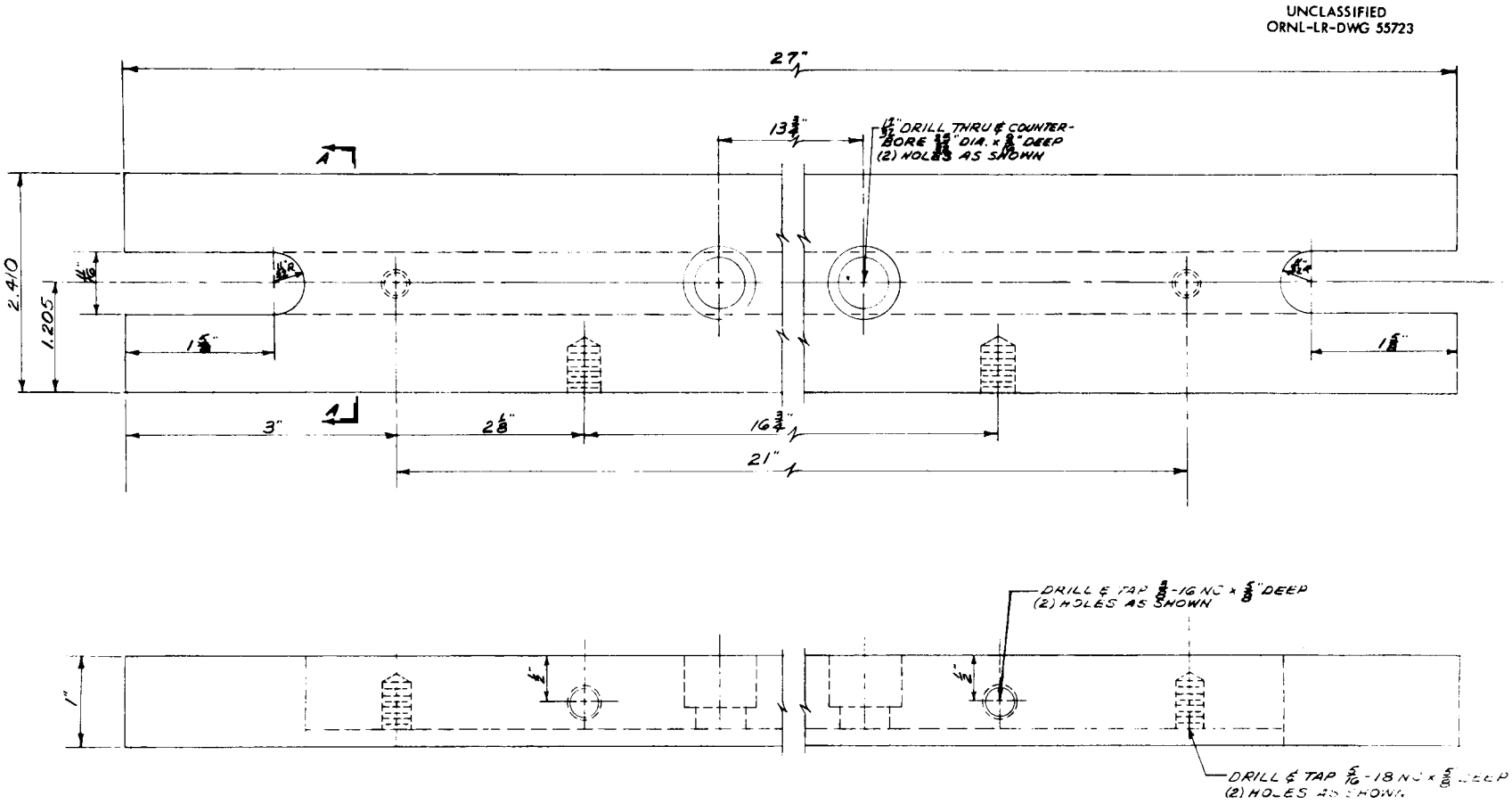

Fig. 30 Machining Jig Base.

UNCLASSIFIED
ORNL-LR-DWG 55718

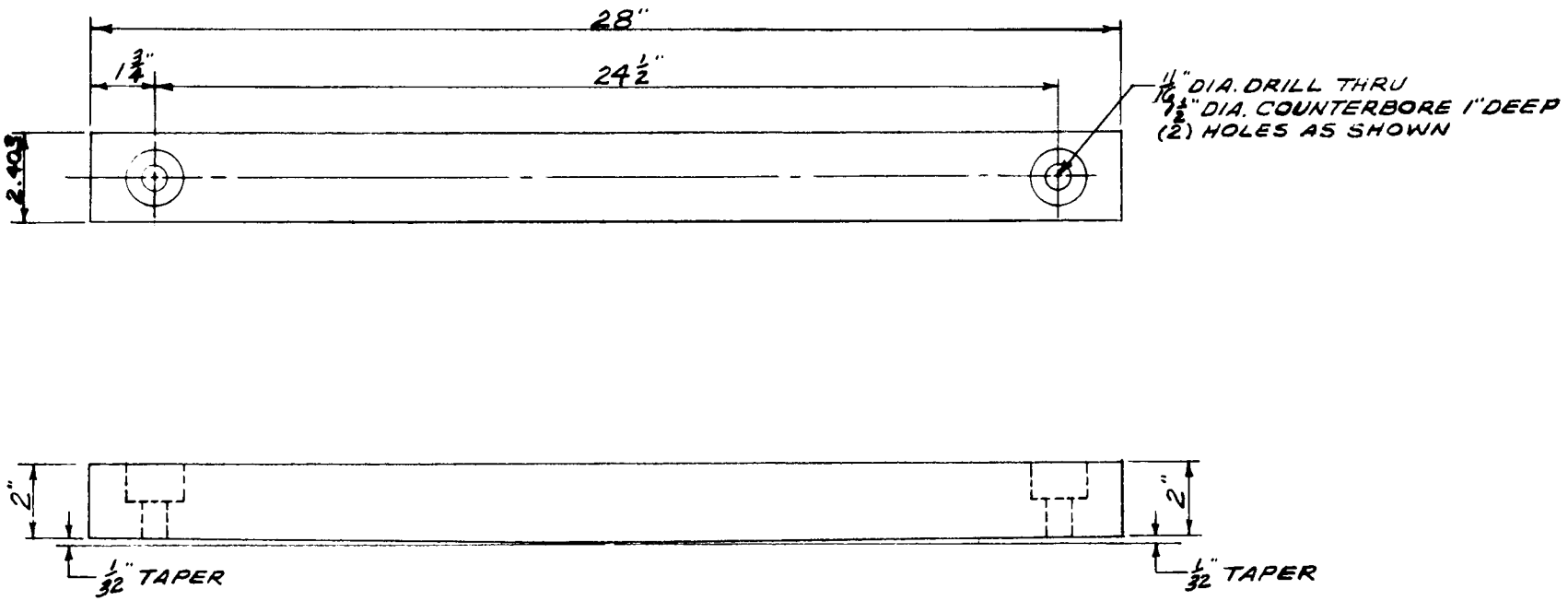

Fig. 31 Hold-Down Bar.

UNCLASSIFIED
ORNL-LR-DWG 55722

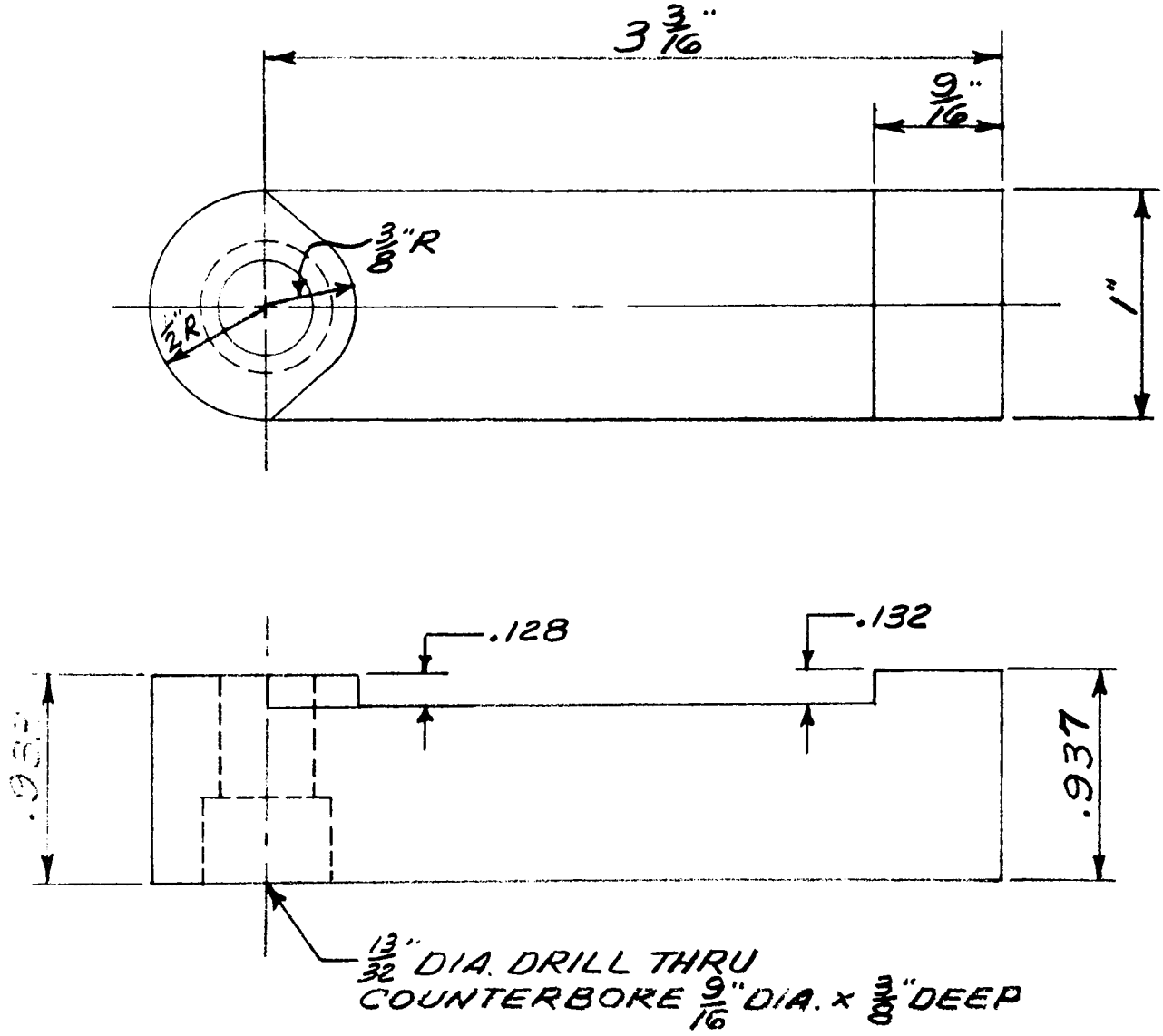

Fig. 32 Side-Positioning Bars.

APPENDIX D

POSITIONING AND MACHINING JIGS APPLICABLE FOR STRADDLE MILLING PLATES MARKED ACCORDING TO SCHEME 2

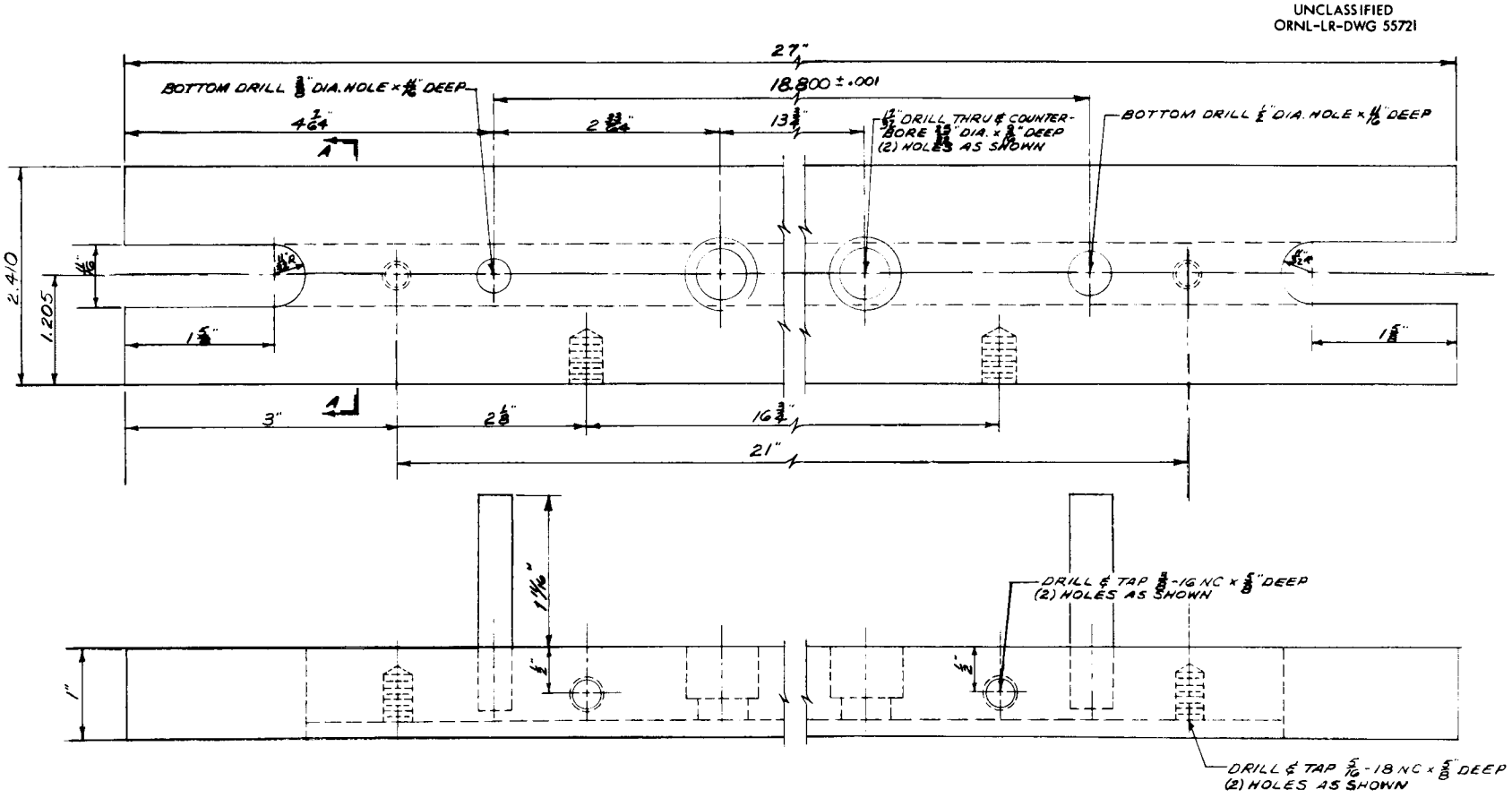

Fig. 33 Machining Jig Base.

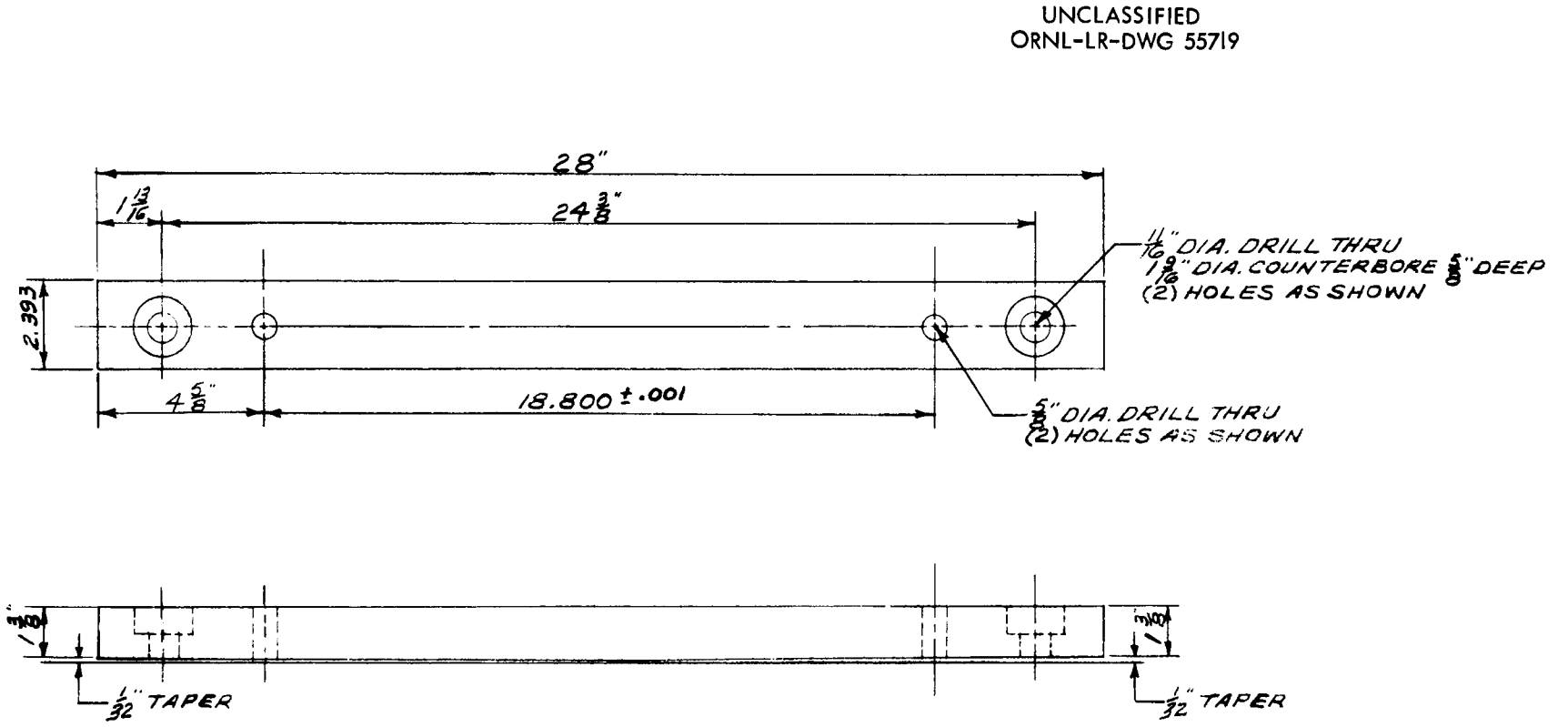

Fig. 34 Hold-Down Bar.

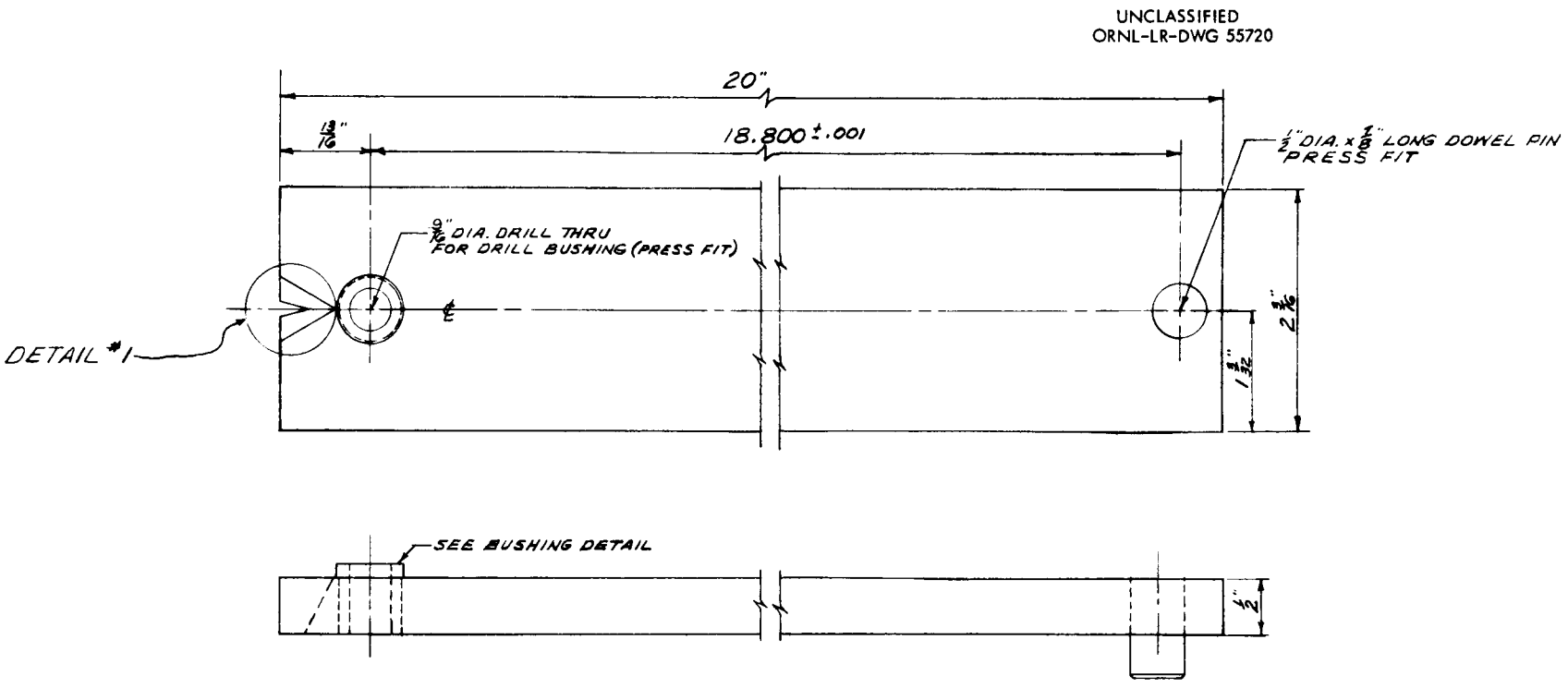

Fig. 35 Positioning Jig.

APPENDIX E

FLAT ANNEALING PLATENS FOR TYPE II FUEL PLATES

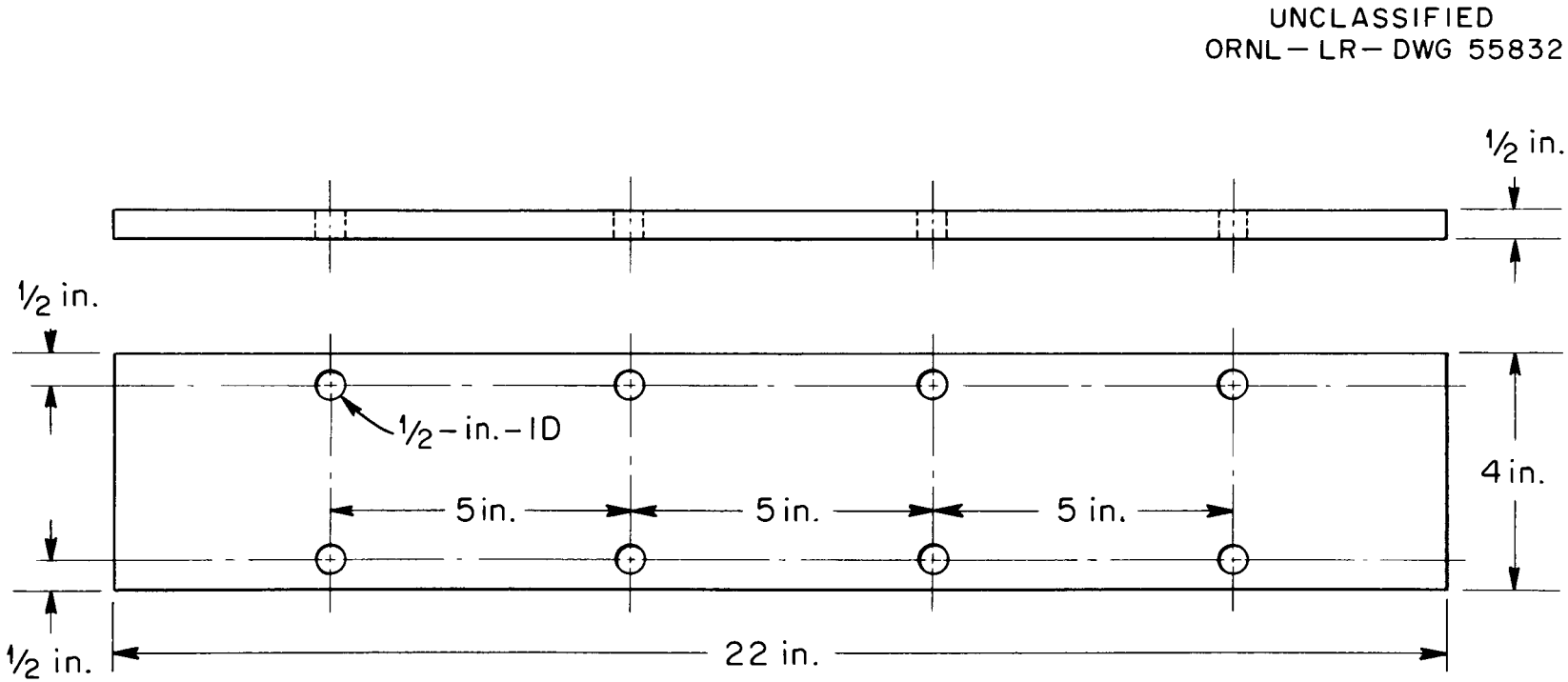

Fig. 36 Flat Annealing Platen.

APPENDIX F

PROBABILITY CALCULATIONS

PROBABILITY CALCULATIONS

Objective:

To determine the probability of any pit intersecting a UO_2 particle.

Assumptions:

1. Uranium dioxide particles are uniformly distributed throughout the matrix so that the probability of locating a particle at any point, P_{UO_2}, is equal to its volume fraction.

2. The frequency-pit depth distribution of pits greater than 50 μ in depth can be described by a truncated exponential distribution function:

$$p(x) = \frac{1}{\theta} e^{-(x - T)\frac{1}{\theta}}$$

where x = depth of pit in microns

T = point of truncation = 50 μ

$\theta = \bar{x} - T$, where $\bar{x}$ is average pit depth

$\bar{x}$ (from data) = 68.44 μ

3. The cross sectional area of the pits is small. The pits can be approximated by a line of appropriate length.

Calculations:

The probability of a pit intersecting a UO_2 particle is given by:

$$P_1 = P \text{ (intersection with a given pit)} = P_{UO_2} \int_a^b \frac{1}{\theta} e^{-\frac{1}{\theta}(x - T)} dx$$

where a = nominal clad thickness

b = nominal thickness of the fuel section (approx 2590 μ).

Then

Clad Thickness (mils)	P_1
5	0.004
4	0.015
3	0.060

If the number of pits deeper than 50 μ per unit plate area assumes a Poisson distribution

$$P_2 = P \text{ (M pits per plate)} = \frac{e^{-\lambda} \lambda^M}{M!}$$

where λ = average number of pits per plate

then

$$P_3 = P \text{ (intersections per plate)} = \frac{e^{-\lambda} \lambda^M}{M!} P_1$$

and, at a 0.005-in.-thick plate cladding:

M	P_3*
0	0.0007
1	0.0012
2	0.0010
3	0.0006
4	0.0003
5	0.0001
6	0.00003

*$\lambda = 1.8$

APPENDIX G

SUMMARY OF SUGGESTED FABRICATION PROCEDURES

SUMMARY OF SUGGESTED FABRICATION PROCEDURES

Preparation of Fuel Compacts

A. Materials

1. Uranium Dioxide
   a. Shape: spheroidal
   b. Size: -100 +140 mesh (105–149 μ)
   c. Porosity: no greater than that illustrated in Fig. 4c
   d. Weight per compact: 96.51 g (approximate - depends on enrichment in U^{235})
2. Stainless Steel Powder
   a. Type: type 347 with 2% silicon addition (similar to type 302B)
   b. Shape: irregular
   c. Size: 100% less than -100 mesh; 70% greater than 325 mesh
   d. Weight per compact: 171.4 g (approximate)

B. Weighing of UO_2 and Stainless Steel Powders

1. Weight to ± 0.03%
2. Add UO_2 to the 4-oz weighing jar containing the stainless steel

C. Blending of Weighed Powder Mixture

1. Place approx 12 jars in a blender which rotates with an oblique rotary motion
2. Blend without any addition for 1/2 hr
3. Add 0.15 cc of 5% paraffin in CCl_4 with an atomizer
4. Reblend for 1-1/2 hr
5. Add 7 cc of 5% paraffin in CCl_4
6. Reblend for 1/2 hr

D. Consolidation of Blended Powders

1. Distribute blended mixture into 2.060-in. x 2.795-in. cavity of die designed in accordance with details in Appendix A
2. Press mixture at 33 tsi

E. Storage of Compacts

1. Store compacts in a vacuum desiccator for 18–24 hr prior to sintering to allow evaporation of most of volatiles

F. Sintering of Compacts

1. Sinter in furnace equipped with a cooling chamber
2. Place fuel compacts in austenitic stainless steel sintering boat with 1/4-in. spacing between compacts
3. Sinter at 1225°C for 75 min in hydrogen (-60°F inlet dew point)
4. Cool sintered compacts in cooling chamber

G. Weighing of Compacts

1. After sintering, weigh each compact to ± 0.03%

H. Coining of Compacts

1. Coin compact at 43 tsi in die as shown in Appendix A

I. Inspection of Coined Compacts

1. Measure thickness of each coined compact with a micrometer in three locations along a diagonal. If the thickness variations are excessive, the compact is subject to rejection.
2. Visually examine for imperfections such as nicked corners and excessive oxidation. Cores with any of these defects are subject to rejection or resintering.

Preparation of Billets

A. Frame

1. Material: type 347 stainless steel sand casting (ASTM Designation: A351 – 58 T Grade CF 8 C)
   (Class I radiographic inspection required)
2. Design
   a. Machine sand cast blank to size shown in Fig. 18
   b. Machine insert from wrought type 347 stainless steel to size shown in Fig. 18

B. Cover Plates

1. Material: wrought type 347 stainless steel
2. Size: 4-3/16 in. x 8-1/16 in. x 0.039 in. (tolerance on thickness is ± 0.0005)

C. Evacuation Tube

1. Material: wrought type 347 stainless steel
2. Size: 1/4-in.-i.d. x 8 in. long

D. Assembly of Billet Components

1. Weld evacuation tube to frame by TID fusion welding
2. Wire brush the mating surfaces of the frame and cover plates with an austenitic stainless steel wire brush
3. Insert two coined compacts in each cavity of the frame (four compacts per billet)
4. Weld cover plates to the frame by fusion welding
5. Check welds for leaks by placing billet (pressurizing with air at 15 psig) under water
6. Evacuate billets to less than 1-μ pressure
7. Seal tube by hot forging while billet is evacuated

Fabrication of Composite Fuel Plates

A. Initial Preheating

1. Preheat evacuated and sealed billet in air at 600°C for 3/4 hr

B. Preheating Prior to Hot Rolling

1. Preheat in open mouth muffle purged with hydrogen (-30°F inlet dew point) at 1200°C for 3/4 hr

C. Hot Rolling

1. Equipment: 20-in.-diam x 30-in.-face 2-high Mesta Mill
2. Reduction in thickness based on mill settings
   a. First two passes: 10% reduction
   b. Balance of passes to thickness of 0.118 in./0.120 in: 25% reduction
   c. Final hot passes at constant mill setting to thickness of 0.114/0.119 in.
   d. Rotate plate about its longitudinal and transverse axes after each pass

3. Reheating between passes
   a. Temperature: 1200°C
   b. Time: 5 min

D. Removal of Surface Oxide

1. Remove all traces of the surface oxide by immersion and agitation in a room-temperature aqueous solution of 5% HF and 15% HNO_3

E. Shearing of Hot-Rolled Plate

1. Shear plate to approx 21 in.

F. Cold Finishing

1. Equipment: 20-in.-diam x 30-in.-face 2-high Mesta Mill
2. Lubricant: SAE 90 oil
3. Reduction in thickness based on mill settings
   a. All passes less than 1% reduction in thickness per pass
4. Rotate plate about its longitudinal and transverse axes after each pass

G. Shearing of Cole Rolled Plate

1. Shear plate to 3 in. x 21 in.

Inspection of Cold-Rolled Plates

A. Measure depth of surface pits with Zeiss Light Section Microscope

B. Radiograph to determine fuel section dimensions and homogeneity of UO_2

Marking of Plates

A. Mark fuel plates in accordance with procedures described in Fig. 26

Machining of Plates

A. Drill and mill a 0.5015 ± 0.0005-in.-hole in each plate individually at location marked at the end of the fuel section.

B. Insert locating device shown in Appendix D in the hole and locate position at opposite end of plate beyond the fuel section for drilling second hole.

C. Drill an 0.375-in.-diam hole at this location.

D. Stack plates, 12 at a time, in the straddle machining jig shown in Appendix D.

E. Position hold-down bar shown in Appendix D.

F. Straddle machine to specified width.

G. Mill plates to specified length.

Degreasing

A. Degrease the plates in trichloroethylene vapor until no evidence of grease remains.

Leaching of the UO_2 from the Surfaces of the Drilled Hole

A. Remove the UO_2 from the exposed surfaces of the hole by immersion of the plates in 50% HNO_3 for 20 min with intermittent agitation of the plates during this period.

Water Rinsing

A. Rinse the plates in turbulent hot (70°C) water to remove all traces of acid and air dry.

Flatten Annealing

A. Coat both sides of each fuel plate with a 5% levigated alumina suspended in water.

B. Stack 14 plates between two 1/2-in.-thick stainless steel platens of the design shown in Appendix E.

C. Bolt platens together.

D. Insert plates in the furnace at 200°C. Purge the furnace with helium until the temperature has exceeded 650°C and introduce hydrogen at -60°F inlet dew point. Heat at a rate of 400°C/hr to 1150°C. Hold 2 hr at this temperature. Furnace cool to 650°C, purge with helium, and, when temperature decreases to 300°C, remove plates from furnace.

E. Remove plates from the platens and scrub alumina from the plates in a tank of water.

F. Rinse plates in hot (70°C) water and air dry.

Final Inspection

A. Radiograph to ensure that the fuel section is properly centered in the plate.

B. Visually examine for surface damage.

C. Make final dimensional measurements.

ORNL-3077
Metals, Ceramics, and Materials
TID-4500 (16th ed.)

DISTRIBUTION

1. C. E. Center
2. Biology Library
3. Health Physics Library
4. Metallurgy Library
5. Central Research Library
6. Reactor Division Library
7. ORNL - Y-12 Technical Library, Document Reference Section
8–13. Laboratory Records
14. Laboratory Records, RC
15. J. P. Murray (K-25)
16. R. G. Jordan (Y-12)
17. G. M. Adamson, Jr.
18. R. J. Beaver
19. D. S. Billington
20. A. L. Boch
21. E. G. Bohlmann
22. E. S. Bomar, Jr.
23. B. S. Borie
24. C. J. Borkowski
25. D. T. Bourgette
26. R. B. Briggs
27. J. A. Burka
28. R. A. Charpie
29–34. J. H. Cherubini
35. R. S. Cockreham
36. W. C. Colwell
37. F. L. Culler
38. J. E. Cunningham
39. R. G. Donnelly
40. D. A. Douglas, Jr.
41. J. H. Erwin
42. A. P. Fraas
43. J. H Frye, Jr.
44. M. M. Goff
45. R. J. Gray
46. W. R. Grimes
47. E. E. Gross
48. J. P. Hammond
49. W. O. Harms
50. T. Hikido
51–55. M. R. Hill
56. A. Hollaender
57. A. S. Householder
58. H. Inouye
59. W. H. Jordan
60. C. P. Keim
61. M. T. Kelley
62. W. J. Kucera
63. R. W. Laing
64. J. T. Lamartine
65. J. A. Lane
66. S. C. Lind
67. R. S. Livingston
68. A. L. Lotts
69. H. G. MacPherson
70. W. D. Manly
71. M. M. Martin
72. W. R. Martin
73. A. J. Miller
74. E. C. Miller
75. K. Z. Morgan
76. R. W. McClung
77. C. J. McHargue
78. M. L. Nelson
79. P. Patriarca
80. D. Phillips
81. S. A. Rabin
82. P. M. Reyling
83. T. K. Roche
84. H. W. Savage
85. L. D. Schaffer
86. J. L. Scott
87. H. E. Seagren
88. J. D. Sease
89. E. D. Shipley
90. M. J. Skinner
91. C. O. Smith
92. A. H. Snell
93. G. M. Slaughter
94. J. A. Swartout
95. R. W. Swindeman
96. E. H. Taylor
97. D. B. Trauger
98. W. C. Thurber
99. T. D. Watts
100. A. M. Weinberg
101. J. C. Wilson
102. C. E. Winters
103. J. L. Gregg (consultant)
104. J. H. Koenig (consultant)
105. R. S. Mateer (consultant)
106. C. S. Smith (consultant)
107. R. Smoluchowski (consultant)
108. H. A. Wilhelm (consultant)

EXTERNAL DISTRIBUTION

109. W. H. Jens, APDA
110–139. A. A. Shoudy, APDA
140. R. C. Williams, APDA
141. L. A. Redecke, AEC, COO
142–143. Bruce Anderson, AEC, COO
144–145. A. L. Benson, AEC, ORO0
146–147. G. M. Wensch, AEC, Washington
148. Donald K. Stevens, Metallurgy and Materials Branch, AEC, Washington
149–730. Given distribution as shown in TID-4500 (16th ed.) under Metals, Ceramics, and Materials Category (75 copies - OTS)
731. Division of Research and Development, AEC, ORO